

## A generalized dimension-reduction method for multidimensional integration in stochastic mechanics

H. Xu and S. Rahman\*,†

*Department of Mechanical and Industrial Engineering, The University of Iowa, Iowa City, IA 52242, U.S.A.*

### SUMMARY

A new, generalized, multivariate dimension-reduction method is presented for calculating statistical moments of the response of mechanical systems subject to uncertainties in loads, material properties, and geometry. The method involves an additive decomposition of an  $N$ -dimensional response function into at most  $S$ -dimensional functions, where  $S \ll N$ ; an approximation of response moments by moments of input random variables; and a moment-based quadrature rule for numerical integration. A new theorem is presented, which provides a convenient means to represent the Taylor series up to a specific dimension without involving any partial derivatives. A complete proof of the theorem is given using two lemmas, also proved in this paper. The proposed method requires neither the calculation of partial derivatives of response, as in commonly used Taylor expansion/perturbation methods, nor the inversion of random matrices, as in the Neumann expansion method. Eight numerical examples involving elementary mathematical functions and solid-mechanics problems illustrate the proposed method. Results indicate that the multivariate dimension-reduction method generates convergent solutions and provides more accurate estimates of statistical moments or multidimensional integration than existing methods, such as first- and second-order Taylor expansion methods, statistically equivalent solutions, quasi-Monte Carlo simulation, and the fully symmetric interpolatory rule. While the accuracy of the dimension-reduction method is comparable to that of the fourth-order Neumann expansion method, a comparison of CPU time suggests that the former is computationally far more efficient than the latter. Copyright © 2004 John Wiley & Sons, Ltd.

**KEY WORDS:** statistical moments; multidimensional integration; dimension reduction; stochastic mechanics; moment-based quadrature; stochastic finite element and meshless methods

### 1. INTRODUCTION

Many problems in computational statistics and stochastic mechanics involve calculating a multidimensional integral to determine the probabilistic characteristics of random output when

\*Correspondence to: S. Rahman, Department of Mechanical and Industrial Engineering, The University of Iowa, Iowa City, IA 52242, U.S.A.

†E-mail: rahman@engineering.uiowa.edu

Contract/grant sponsor: U.S. National Science Foundation; contract/grant number: CMS-9733058, CMS-9900196 and DMI-0355487

Contract/grant sponsor: U.S. Army sponsored Automotive Research Centre

*Received 3 September 2003*

*Revised 5 April 2004*

*Accepted 7 May 2004*

input uncertainties are characterized either partially by moments or fully by probability density functions [1–6]. Current stochastic methods used to calculate this integral comprise three major approaches: (1) analytical methods, (2) simulation methods, and (3) numerical integration. Analytical methods, which include Taylor expansion or perturbation methods [7–10], the Neumann expansion method [11–15], the decomposition method [16, 17], the polynomial chaos expansion method [14], the statistically equivalent solution [18], the point estimate method [19] and others [1], are traditionally employed to predict second-moment characteristics of random output. Presented in Reference [20], a brief review suggests that most analytical methods are computationally inefficient or less accurate when the input–output relationship is highly non-linear or when the number and/or uncertainty of input random variables is large. Simulation and sampling methods, such as direct Monte Carlo simulation [21], quasi-Monte Carlo simulation [22–24], importance sampling [25, 26], directional simulation [27, 28], and others [29–32], are well known in the statistics and reliability literature. While simulation methods do not exhibit the limitations of analytical methods, they generally require considerably more extensive calculations than analytical methods. Consequently, simulation methods are useful when alternative methods are inapplicable or inaccurate, and have been traditionally employed as a yardstick for evaluating analytical methods. Methods involving numerical integration have also been employed to calculate statistical properties of output. Various quadrature rules, such as Gauss–Legendre, Gauss–Hermite, and others, can be utilized. In recent years, new interpolatory rules have also been developed to evaluate the integral more accurately and efficiently [4–6]. Nevertheless, numerical integration is not economically feasible when (1) the number of input random variables exceeds three or four and (2) expensive calculation of the output variable is required. Hence, new stochastic methods that can handle arbitrarily large non-linearity, many random variables, and arbitrarily large uncertainties of input, and yet predict both response moments and reliability accurately, are highly desirable.

Recently, the authors proposed a univariate dimension-reduction method [20] for calculating statistical moments of the response of mechanical systems subject to uncertainties in loads, material properties, and geometry. This univariate method involves an additive decomposition of a multidimensional response function into multiple one-dimensional functions; an approximation of response moments by moments of single random variables; and a moment-based quadrature rule for numerical integration. The resultant moment equations entail evaluation of  $N$  one-dimensional integrals, which is substantially simpler and more efficient than performing one  $N$ -dimensional integration. Numerical results involving small to moderate uncertainties of input, presented in Reference [20], indicate that the univariate dimension-reduction method provides more accurate estimates of statistical moments or multidimensional integration than most existing methods. However, for a system with arbitrarily large random variation and/or high non-linearity, the univariate dimension reduction may not be adequate due to two- and other higher-dimensional integrations contained in the residual error of this method. The error can be reduced further, for example in the bivariate dimension-reduction method, if terms associated with bivariate integrations are retained in approximating the response. However, this process requires two-dimensional integrations, as opposed to one-dimensional integrations in the univariate method. Nevertheless, it is conceivable that bivariate and, in general, multivariate dimension-reduction methods can be developed to reduce residual error to an arbitrarily small value, which is the subject of the current paper.

This paper presents a new, generalized dimension-reduction method for predicting second-moment characteristics of the response of mechanical systems subject to random loads, material

properties, and geometry. The method involves an additive decomposition of an  $N$ -dimensional response function into 1-, 2-, ...,  $S$ -dimensional functions, where  $S \ll N$ ; an approximation of response moments by moments of input random variables; and a moment-based quadrature rule for numerical integration. A new theorem is presented, which provides a convenient means of representing the Taylor series up to a specific dimension without needing to know any derivatives. A complete proof of the theorem is given using two lemmas, also proved in this paper. Finally, two sets of numerical examples illustrate the accuracy, computational efficiency, and convergence of the proposed method.

## 2. BIVARIATE DIMENSION-REDUCTION METHOD

Consider a continuous, differentiable, real-valued function  $y(\mathbf{x})$  or  $y(x_1, \dots, x_N)$  that depends on  $N$  independent variables  $\mathbf{x} = \{x_1, \dots, x_N\}^T \in \mathfrak{R}^N$ . Let

$$I[y(\mathbf{x})] \equiv \int_{-1}^1 \cdots \int_{-1}^1 y(\mathbf{x}) \, d\mathbf{x} \quad (1)$$

denote an  $N$ -dimensional integration of  $y(\mathbf{x})$  on a symmetric domain  $[-1, 1]^N$ . If the Taylor series expansion of  $y(\mathbf{x})$  at  $\mathbf{x} = \mathbf{0} = \{0, \dots, 0\}^T$ , expressed by

$$\begin{aligned} y(\mathbf{x}) = & y(\mathbf{0}) + \sum_{j=1}^{\infty} \frac{1}{j!} \sum_{i=1}^N \frac{\partial^j y}{\partial x_i^j}(\mathbf{0}) x_i^j \\ & + \sum_{j_2=1}^{\infty} \sum_{j_1=1}^{\infty} \frac{1}{j_1! j_2!} \sum_{i_1 < i_2} \frac{\partial^{j_1+j_2} y}{\partial x_{i_1}^{j_1} \partial x_{i_2}^{j_2}}(\mathbf{0}) x_{i_1}^{j_1} x_{i_2}^{j_2} \\ & + \sum_{j_3=1}^{\infty} \sum_{j_2=1}^{\infty} \sum_{j_1=1}^{\infty} \frac{1}{j_1! j_2! j_3!} \sum_{i_1 < i_2 < i_3} \frac{\partial^{j_1+j_2+j_3} y}{\partial x_{i_1}^{j_1} \partial x_{i_2}^{j_2} \partial x_{i_3}^{j_3}}(\mathbf{0}) x_{i_1}^{j_1} x_{i_2}^{j_2} x_{i_3}^{j_3} + \cdots \end{aligned} \quad (2)$$

is substituted in Equation (1), the integral becomes

$$\begin{aligned} I[y(\mathbf{x})] = & I[y(\mathbf{0})] + \sum_{j=1}^{\infty} \frac{1}{j!} \sum_{i=1}^N \frac{\partial^j y}{\partial x_i^j}(\mathbf{0}) I[x_i^j] \\ & + \sum_{j_2=1}^{\infty} \sum_{j_1=1}^{\infty} \frac{1}{j_1! j_2!} \sum_{i_1 < i_2} \frac{\partial^{j_1+j_2} y}{\partial x_{i_1}^{j_1} \partial x_{i_2}^{j_2}}(\mathbf{0}) I[x_{i_1}^{j_1} x_{i_2}^{j_2}] \\ & + \sum_{j_3=1}^{\infty} \sum_{j_2=1}^{\infty} \sum_{j_1=1}^{\infty} \frac{1}{j_1! j_2! j_3!} \sum_{i_1 < i_2 < i_3} \frac{\partial^{j_1+j_2+j_3} y}{\partial x_{i_1}^{j_1} \partial x_{i_2}^{j_2} \partial x_{i_3}^{j_3}}(\mathbf{0}) I[x_{i_1}^{j_1} x_{i_2}^{j_2} x_{i_3}^{j_3}] + \cdots \end{aligned} \quad (3)$$

Now consider two Taylor series expansions of the univariate function  $y(0, \dots, 0, x_i, 0, \dots, 0)$  at  $x_i = 0$  and the bivariate function  $y(0, \dots, 0, x_{i_1}, 0, \dots, 0, x_{i_2}, 0, \dots, 0)$  at  $x_{i_1} = x_{i_2} = 0$ ,

yielding

$$y(0, \dots, 0, x_i, 0, \dots, 0) = y(\mathbf{0}) + \sum_{j=1}^{\infty} \frac{1}{j!} \frac{\partial^j y}{\partial x_i^j}(\mathbf{0}) x_i^j \tag{4}$$

$$y(0, \dots, 0, x_{i_1}, 0, \dots, 0, x_{i_2}, 0, \dots, 0) = y(\mathbf{0}) + \sum_{j=1}^{\infty} \frac{1}{j!} \frac{\partial^j y}{\partial x_{i_1}^j}(\mathbf{0}) x_{i_1}^j + \sum_{j=1}^{\infty} \frac{1}{j!} \frac{\partial^j y}{\partial x_{i_2}^j}(\mathbf{0}) x_{i_2}^j + \sum_{j_1=1}^{\infty} \sum_{j_2=1}^{\infty} \frac{1}{j_1! j_2!} \frac{\partial^{j_1+j_2} y}{\partial x_{i_1}^{j_1} \partial x_{i_2}^{j_2}}(\mathbf{0}) x_{i_1}^{j_1} x_{i_2}^{j_2} \tag{5}$$

Summation of these two expansions with respect to  $i$  and  $i_1 < i_2$ , respectively, gives

$$\sum_{i=1}^N y(0, \dots, 0, x_i, 0, \dots, 0) = N y(\mathbf{0}) + \sum_{i=1}^N \sum_{j=1}^{\infty} \frac{1}{j!} \frac{\partial^j y}{\partial x_i^j}(\mathbf{0}) x_i^j \tag{6}$$

$$\sum_{i_1 < i_2} y(0, \dots, 0, x_{i_1}, 0, \dots, 0, x_{i_2}, 0, \dots, 0) = \frac{N(N-1)}{2} y(\mathbf{0}) + (N-1) \sum_{i=1}^N \sum_{j=1}^{\infty} \frac{1}{j!} \frac{\partial^j y}{\partial x_i^j}(\mathbf{0}) x_i^j + \sum_{i_1 < i_2} \sum_{j_1=1}^{\infty} \sum_{j_2=1}^{\infty} \frac{1}{j_1! j_2!} \frac{\partial^{j_1+j_2} y}{\partial x_{i_1}^{j_1} \partial x_{i_2}^{j_2}}(\mathbf{0}) x_{i_1}^{j_1} x_{i_2}^{j_2} \tag{7}$$

Now consider a bivariate approximation

$$\hat{y}(\mathbf{x}) \equiv \sum_{i_1 < i_2} y(0, \dots, 0, x_{i_1}, 0, \dots, 0, x_{i_2}, 0, \dots, 0) - (N-2) \sum_{i=1}^N y(0, \dots, 0, x_i, 0, \dots, 0) + \frac{(N-1)(N-2)}{2} y(\mathbf{0}) \tag{8}$$

of  $y(\mathbf{x})$ , where each term on the right-hand side is a function of at most two variables. The integration of  $\hat{y}(\mathbf{x})$  is then

$$I[\hat{y}(\mathbf{x})] = \sum_{i_1 < i_2} I[y(0, \dots, 0, x_{i_1}, 0, \dots, 0, x_{i_2}, 0, \dots, 0)] - (N-2) \sum_{i=1}^N I[y(0, \dots, 0, x_i, 0, \dots, 0)] + \frac{(N-1)(N-2)}{2} I[y(\mathbf{0})] \tag{9}$$

Substituting Equations (6) and (7) into (9), and subsequently applying the integration operator, yields

$$I[\hat{y}(\mathbf{x})] = I[y(\mathbf{0})] + \sum_{i=1}^N \sum_{j=1}^{\infty} \frac{1}{j!} \frac{\partial^j y}{\partial x_i^j}(\mathbf{0}) I[x_i^j] + \sum_{i_1 < i_2} \sum_{j_1=1}^{\infty} \sum_{j_2=1}^{\infty} \frac{1}{j_1! j_2!} \frac{\partial^{j_1+j_2} y}{\partial x_{i_1}^{j_1} \partial x_{i_2}^{j_2}}(\mathbf{0}) I[x_{i_1}^{j_1} x_{i_2}^{j_2}] \tag{10}$$

Note that Equation (3) contains all terms on the right-hand side of Equation (10), resulting in a residual error of

$$I[y(\mathbf{x})] - I[\hat{y}(\mathbf{x})] = \sum_{j_3=1}^{\infty} \sum_{j_2=1}^{\infty} \sum_{j_1=1}^{\infty} \frac{1}{j_1!j_2!j_3!} \sum_{i_1 < i_2 < i_3} \frac{\partial^{j_1+j_2+j_3} y}{\partial x_{i_1}^{j_1} \partial x_{i_2}^{j_2} \partial x_{i_3}^{j_3}}(\mathbf{0}) I \left[ x_{i_1}^{j_1} x_{i_2}^{j_2} x_{i_3}^{j_3} \right] + \dots \quad (11)$$

which includes contributions from integrations of only dimensions three and higher. If partial derivatives  $\partial^{j_1+j_2+j_3} y(\mathbf{0}) / \partial x_{i_1}^{j_1} \partial x_{i_2}^{j_2} \partial x_{i_3}^{j_3}$  are negligibly small,  $I[\hat{y}(\mathbf{x})]$  in Equation (10) provides a convenient approximation of  $I[y(\mathbf{x})]$ . Note that  $I[\hat{y}(\mathbf{x})]$  represents a reduced integration, since only one- and two-dimensional integrations are required, as opposed to one  $N$ -dimensional integration in  $I[y(\mathbf{x})]$ . There is no need to calculate partial derivatives. Since each term of the integrand in  $I[\hat{y}(\mathbf{x})]$  has at most two variables, this approximation is called the bivariate dimension-reduction method. Furthermore, Equation (10) yields exact results when  $y(\mathbf{x}) = \sum_{i < j} y_{ij}(x_i, x_j)$ , i.e. when  $y(\mathbf{x})$  can be additively decomposed into functions  $y_{ij}(x_i, x_j)$  of at most two variables.

In order to integrate over a general non-symmetric domain  $\prod_{i=1}^N [a_i, b_i]$ , such as

$$I[y(\mathbf{x})] = \int_{a_N}^{b_N} \dots \int_{a_1}^{b_1} y(x_1, \dots, x_N) dx_1 \dots dx_N \quad (12)$$

where  $-\infty \leq a_i \leq \infty$  and  $-\infty \leq b_i \leq \infty$ , a linear transformation

$$x_i = \frac{b_i + a_i}{2} + \frac{b_i - a_i}{2} \xi_i, \quad i = 1, \dots, N \quad (13)$$

maps the original integral over a non-symmetric domain to

$$I[y(\mathbf{x})] = \prod_{i=1}^N \frac{b_i - a_i}{2} \int_{-1}^1 \dots \int_{-1}^1 \eta(\xi_1, \dots, \xi_N) d\xi_1 \dots d\xi_N \quad (14)$$

which represents an integral over a symmetric domain where  $\eta(\xi_1, \dots, \xi_N)$  is the transformed function due to a change of variables from  $\mathbf{x}$  to  $\xi$ -space. Hence, Equation (11) is applicable to multidimensional integrations over non-symmetric domains as well.

### 3. GENERALIZED DIMENSION-REDUCTION METHOD

The bivariate dimension-reduction method described in the previous section can be generalized to reduce the residual error to an arbitrarily small value. To accomplish this generalization, a new theorem associated with the Taylor series is presented, which provides a convenient means to represent the Taylor series up to a specific dimension without specific knowledge of any derivatives. The theorem is proven using two lemmas, also proven herein, as follows.

*Lemma 1*

For any  $N$ -dimensional function  $y(x_1, \dots, x_N)$  having convergent Taylor series, let  $T(y, N) = \sum_{i=0}^N t_i$  represent the Taylor series expansion of  $y(x_1, \dots, x_N)$  at  $\mathbf{x} = \mathbf{0}$ , where  $t_i, 0 \leq i \leq N$ , is

the summation of all terms with  $i$  variables, i.e.

$$\begin{aligned}
 t_0 &= y(\mathbf{0}) \\
 t_1 &= \sum_{j_1} \frac{1}{j_1!} \sum_{i_1=1}^N \frac{\partial^{j_1} y}{\partial x_{i_1}^{j_1}}(\mathbf{0}) x_{i_1}^{j_1} \\
 t_2 &= \sum_{j_1, j_2} \frac{1}{j_1! j_2!} \sum_{i_1 < i_2} \frac{\partial^{j_1+j_2} y}{\partial x_{i_1}^{j_1} \partial x_{i_2}^{j_2}}(\mathbf{0}) x_{i_1}^{j_1} x_{i_2}^{j_2} \\
 &\vdots \\
 t_N &= \sum_{j_1, j_2, \dots, j_N} \frac{1}{j_1! j_2! \dots j_N!} \sum_{i_1 < i_2 < \dots < i_N} \frac{\partial^{j_1+j_2+\dots+j_N} y}{\partial x_{i_1}^{j_1} \partial x_{i_2}^{j_2} \dots \partial x_{i_N}^{j_N}}(\mathbf{0}) x_{i_1}^{j_1} x_{i_2}^{j_2} \dots x_{i_N}^{j_N}
 \end{aligned} \tag{15}$$

If

$$y_R = \sum_{k_1 < k_2 < \dots < k_R} y(0, \dots, 0, x_{k_1}, 0, \dots, 0, x_{k_2}, 0, \dots, 0, x_{k_R}, 0, \dots, 0), \quad 0 \leq R \leq N \tag{16}$$

defines a summation of terms that contain at most  $R$  variables, then

$$y_R = \sum_{k=0}^R \binom{N-k}{R-k} t_k \tag{17}$$

*Proof*

Using Taylor expansion at  $x_{k_1} = x_{k_2} = \dots = x_{k_R} = 0$ ,

$$\begin{aligned}
 &y(0, \dots, 0, x_{k_1}, 0, \dots, 0, x_{k_2}, 0, \dots, 0, x_{k_3}, 0, \dots, 0, x_{k_R}, 0, \dots, 0) \\
 &= y(\mathbf{0}) + \sum_{j_1} \frac{1}{j_1!} \sum_{i_1=1}^R \frac{\partial^{j_1} y}{\partial x_{i_1}^{j_1}}(\mathbf{0}) x_{i_1}^{j_1} + \sum_{j_1, j_2} \frac{1}{j_1! j_2!} \sum_{i_1 < i_2} \frac{\partial^{j_1+j_2} y}{\partial x_{i_1}^{j_1} \partial x_{i_2}^{j_2}}(\mathbf{0}) x_{i_1}^{j_1} x_{i_2}^{j_2} + \dots \\
 &\quad + \sum_{j_1, j_2, \dots, j_R} \frac{1}{j_1! j_2! \dots j_R!} \sum_{i_1 < i_2 < \dots < i_R} \frac{\partial^{j_1+j_2+\dots+j_R} y}{\partial x_{i_1}^{j_1} \partial x_{i_2}^{j_2} \dots \partial x_{i_R}^{j_R}}(\mathbf{0}) x_{i_1}^{j_1} x_{i_2}^{j_2} \dots x_{i_R}^{j_R}
 \end{aligned} \tag{18}$$

Hence, Equation (16) becomes

$$\begin{aligned}
 y_R &= \sum_{k_1 < k_2 < \dots < k_R} y(0, \dots, 0, x_{k_1}, 0, \dots, 0, x_{k_2}, 0, \dots, 0, x_{k_R}, 0, \dots, 0) \\
 &= \sum_{k_1 < k_2 < \dots < k_R} [y(\mathbf{0})] + \sum_{k_1 < k_2 < \dots < k_R} \left[ \sum_{j_1} \frac{1}{j_1!} \sum_{i_1=1}^R \frac{\partial^{j_1} y}{\partial x_{i_1}^{j_1}}(\mathbf{0}) x_{i_1}^{j_1} \right] \\
 &\quad + \sum_{k_1 < k_2 < \dots < k_R} \left[ \sum_{j_1, j_2} \frac{1}{j_1! j_2!} \sum_{i_1 < i_2} \frac{\partial^{j_1+j_2} y}{\partial x_{i_1}^{j_1} \partial x_{i_2}^{j_2}}(\mathbf{0}) x_{i_1}^{j_1} x_{i_2}^{j_2} \right] + \dots
 \end{aligned}$$

$$\begin{aligned}
 & + \sum_{k_1 < k_2 < \dots < k_R} \left[ \sum_{j_1, j_2, \dots, j_R} \frac{1}{j_1! j_2! \dots j_R!} \sum_{i_1 < i_2 < \dots < i_R} \frac{\partial^{j_1 + j_2 + \dots + j_R} y}{\partial x_{k_{i_1}}^{j_1} \partial x_{k_{i_2}}^{j_2} \dots \partial x_{k_{i_R}}^{j_R}} (\mathbf{0})_{x_{k_{i_1}}^{j_1} x_{k_{i_2}}^{j_2} \dots x_{k_{i_R}}^{j_R}} \right] \\
 & = \sum_{k=0}^R \binom{N-k}{R-k} t_k
 \end{aligned} \tag{19}$$

which completes the proof of Lemma 1. □

*Lemma 2*

For any integers  $S < N$  and  $k \leq S$ ,

$$\sum_{i=0}^{S-k} (-1)^i \binom{N-S+i-1}{i} \binom{N-k}{S-i-k} = 1 \tag{20}$$

*Proof*

If  $k = S$ , proving Lemma 2 is trivial. If  $k < S$ ,

$$\begin{aligned}
 & \sum_{i=0}^{S-k} (-1)^i \binom{N-S+i-1}{i} \binom{N-k}{S-i-k} \\
 & = \sum_{i=0}^{S-k} (-1)^i \frac{(N-S+i-1)!(N-k)!}{i!(N-S-1)!(S-i-k)!(N-S+i)!} \\
 & = \sum_{i=0}^{S-k} (-1)^i \frac{1}{(N-S+i)} \frac{(N-S)(N-k)!(S-k)!}{i!(N-S)!(S-i-k)!(S-k)!} \\
 & = \binom{N-k}{S-k} \sum_{i=0}^{S-k} (-1)^i \frac{(N-S)}{(N-S+i)} \binom{S-k}{i} \\
 & = \binom{N-k}{S-k} \sum_{i=0}^{S-k} (-1)^i \left[ 1 - \frac{i}{(N-S+i)} \right] \binom{S-k}{i}
 \end{aligned} \tag{21}$$

Since

$$\sum_{i=0}^{S-k} (-1)^i \binom{S-k}{i} = (1-1)^{S-k} = 0 \tag{22}$$

Equation (21) simplifies to

$$\begin{aligned}
 & \sum_{i=0}^{S-k} (-1)^i \binom{N-S+i-1}{i} \binom{N-k}{S-i-k} \\
 & = \binom{N-k}{S-k} \sum_{i=0}^{S-k} (-1)^{i+1} \frac{i}{(N-S+i)} \binom{S-k}{i}
 \end{aligned}$$

$$\begin{aligned}
 &= \binom{N-k}{S-k} \sum_{i=0}^{S-k-1} (-1)^i \frac{i+1}{(N-S+i+1)} \binom{S-k}{i+1} \\
 &= \binom{N-k}{S-k} \frac{(S-k)}{(N-S+1)} \sum_{i=0}^{S-k-1} (-1)^i \frac{N-S+1}{(N-S+i+1)} \binom{S-k-1}{i} \\
 &= \binom{N-k}{S-k} \frac{(S-k)}{(N-S+1)} \sum_{i=1}^{S-k-1} (-1)^i \left[ 1 - \frac{i}{(N-S+i+1)} \right] \binom{S-k-1}{i} \\
 &= \binom{N-k}{S-k} \frac{(S-k)}{(N-S+1)} \sum_{i=1}^{S-k-1} (-1)^{i+1} \frac{i}{(N-S+i+1)} \binom{S-k-1}{i} \\
 &= \binom{N-k}{S-k} \frac{(S-k)(S-k-1)}{(N-S+1)(N-S+2)} \sum_{i=0}^{S-k-2} (-1)^i \frac{(N-S+2)}{(N-S+i+2)} \binom{S-k-2}{i} \\
 &= \binom{N-k}{S-k} \frac{(S-k)(S-k-1)\dots 2 \cdot 1}{(N-S+1)(N-S+2)\dots(N-k)} \\
 &= \binom{N-k}{S-k} \frac{(S-k)!(N-S)!}{(N-k)!} = 1
 \end{aligned} \tag{23}$$

which completes the proof of Lemma 2. □

*Theorem*

For any  $N$ -dimensional function  $y(\mathbf{x}) = y(x_1, \dots, x_N)$ , if

$$\hat{y} \equiv \sum_{i=0}^S (-1)^i \binom{N-S+i-1}{i} y_{S-i} \tag{24}$$

represents an  $S$ -variate approximation of  $y(x_1, \dots, x_N)$ , where  $y_0 = y(\mathbf{0})$ ,  $S \leq N$ , and  $y_R$  is already defined in Equation (16), then  $\hat{y}$  consists of all terms of the Taylor series of  $y(x_1, \dots, x_N)$  that have less than or equal to  $S$  variables, i.e.

$$\hat{y} = \sum_{k=0}^S t_k \tag{25}$$

*Proof*

By Lemma 1

$$y_{S-i} = \sum_{k=0}^{S-i} \binom{N-k}{S-i-k} t_k \tag{26}$$

which can be substituted in Equation (24) to obtain

$$\hat{y} = \sum_{i=0}^S \sum_{k=0}^{S-i} (-1)^i \binom{N-S+i-1}{i} \binom{N-k}{S-i-k} t_k \quad (27)$$

Since  $\sum_{i=0}^S \sum_{k=0}^{S-i} = \sum_{k=0}^S \sum_{i=0}^{S-k}$  and invoking Lemma 2, Equation (27) reduces to

$$\hat{y} = \sum_{k=0}^S \sum_{i=0}^{S-k} (-1)^i \binom{N-S+i-1}{i} \binom{N-k}{S-i-k} t_k = \sum_{k=0}^S t_k \quad (28)$$

which completes the proof of the proposed theorem.  $\square$

The proposed theorem implies that the multivariate approximation  $\hat{y}$ , defined in Equation (24), consists of all terms of the Taylor series expansion of  $y(x_1, \dots, x_N)$  that have no more than  $S$  variables. Following application of the integral operator,

$$I[\hat{y}] = \sum_{i=0}^S (-1)^i \binom{N-S+i-1}{i} I[y_{S-i}] \quad (29)$$

which represents a reduced integration, since only 1-, 2-, ...,  $S$ -dimensional integrations are required, as opposed to an  $N$ -dimensional integration in  $I[y]$ . If the integrations of series terms with more than  $S$  variables are negligibly small, Equation (29) provides a convenient approximation of  $I[y]$ . When  $S \ll N$ , the computational effort in evaluating  $I[\hat{y}]$  becomes significantly smaller than evaluating  $I[y]$ . Again, there is no need to calculate partial derivatives. Furthermore, Equation (29) yields exact results when  $y(x_1, \dots, x_N)$  can be additively decomposed into functions of at most  $S$  variables.

#### 4. APPLICATION TO STOCHASTIC PROBLEMS

##### 4.1. Statistical moments of response

Consider a mechanical system subject to a zero-mean independent random input vector  $\mathbf{X} = \{X_1, \dots, X_N\}^T \in \mathfrak{R}^N$ , which characterizes uncertainty in loads, material properties, and geometry. Let  $Y(\mathbf{X})$  represent a relevant response of interest, for which the  $l$ th statistical moment

$$m_l \equiv \mathcal{E}[Y^l(\mathbf{X})] = \int_{\mathfrak{R}^N} y^l(\mathbf{x}) f_{\mathbf{X}}(\mathbf{x}) \, d\mathbf{x} \quad (30)$$

is sought, where  $f_{\mathbf{X}}(\mathbf{x}) = f_{X_1 \dots X_N}(x_1, \dots, x_N)$  is the joint probability density function of  $\mathbf{X}$  and  $\mathcal{E}$  is the expectation operator. If  $Z(\mathbf{X}) = Y^l(\mathbf{X})$ , the  $l$ th moment can also be evaluated from

$$m_l \equiv \mathcal{E}[Z(\mathbf{X})] = \int_{\mathfrak{R}^N} z(\mathbf{x}) f_{\mathbf{X}}(\mathbf{x}) \, d\mathbf{x} \quad (31)$$

Following the  $S$ -variate dimension reduction procedure in Equations (24) and (29), the  $l$ th moment can be approximated by

$$\begin{aligned}
 m_l &\cong \mathcal{E}[\hat{Z}(\mathbf{X})] \\
 &= \sum_{i=0}^S (-1)^i \binom{N-S+i-1}{i} \\
 &\quad \times \sum_{k_1 < k_2 < \dots < k_{S-i}} \mathcal{E}[Z(0, \dots, 0, X_{k_1}, 0, \dots, 0, X_{k_2}, 0, \dots, 0, X_{k_{S-i}}, 0, \dots, 0)] \quad (32)
 \end{aligned}$$

By definition,

$$\begin{aligned}
 &\mathcal{E}[Z(0, \dots, 0, X_{k_1}, 0, \dots, 0, X_{k_2}, 0, \dots, 0, X_{k_{S-i}}, 0, \dots, 0)] \\
 &\equiv \int_{-\infty}^{\infty} z(0, \dots, 0, x_{k_1}, 0, \dots, 0, x_{k_2}, 0, \dots, 0, x_{k_{S-i}}, 0, \dots, 0) f_{\tilde{\mathbf{X}}}(\tilde{\mathbf{x}}) d\tilde{\mathbf{x}} \quad (33)
 \end{aligned}$$

where  $\tilde{\mathbf{x}} = \{x_{k_1}, \dots, x_{k_{S-i}}\}^T \in \mathfrak{R}^{S-i}$ ,  $\tilde{\mathbf{X}} = \{X_{k_1}, \dots, X_{k_{S-i}}\} \in \mathfrak{R}^{S-i}$ , and

$$f_{\tilde{\mathbf{X}}}(\tilde{\mathbf{x}}) = \prod_{j=1}^{S-i} f_{X_{k_j}}(x_{k_j}) \quad (34)$$

is the joint probability density of  $\tilde{\mathbf{X}}$ . Note that Equation (34) is valid for independent random vector  $\tilde{\mathbf{X}}$ . If  $\tilde{\mathbf{X}}$  comprises dependent variables with its joint density  $f_{\tilde{\mathbf{X}}}(\tilde{\mathbf{x}}) = f_{X_1 \dots X_N}(x_1, \dots, x_N)$ , a multivariate transformation such as Rosenblatt transformation [33] should be applied to transform the dependent random vector  $\tilde{\mathbf{X}}$  to an independent standard Gaussian random vector  $\mathbf{U}$ . The Rosenblatt transformation is given by [33]

$$\begin{aligned}
 u_1 &= \Phi^{-1}[F_{X_1}(x_1)] \\
 u_2 &= \Phi^{-1}[F_{X_2}(x_2|x_1)] \\
 &\vdots \\
 u_N &= \Phi^{-1}[F_{X_N}(x_N|x_1, x_2, \dots, x_{N-1})]
 \end{aligned} \quad (35)$$

in which  $F_{X_i}(x_i|x_1, x_2, \dots, x_{i-1})$  is the cumulative distribution function of component  $X_i$  conditional on  $X_1 = x_1, X_2 = x_2, \dots, X_{i-1} = x_{i-1}$  and  $\Phi(\bullet)$  is the cumulative distribution function of a standard Gaussian random variable. The conditional distribution function  $F_{X_i}(x_i|x_1, x_2, \dots, x_{i-1})$  can be obtained from

$$F_{X_i}(x_i|x_1, x_2, \dots, x_{i-1}) = \frac{\int_{-\infty}^{x_i} f_{X_1, X_2, \dots, X_i}(x_1, x_2, \dots, x_{i-1}, s) ds}{f_{X_1, X_2, \dots, X_{i-1}}(x_1, x_2, \dots, x_{i-1})} \quad (36)$$

where  $f_{X_1, X_2, \dots, X_{i-1}}(x_1, x_2, \dots, x_{i-1})$  is the joint probability density function of random vector  $\{X_1, X_2, \dots, X_{i-1}\}^T$ .

Equation (33) only requires at most  $S$ -dimensional deterministic integration, which can be more easily evaluated using standard quadrature rules. For example, Gauss–Legendre and Gauss–Hermite quadratures are frequently used when  $X_j$  follows uniform and Gaussian probability distributions, respectively [34]. For an arbitrary distribution of  $X_j$ , a moment-based quadrature rule, described in authors' previous work [20], can be used to evaluate the integral. Appendix A provides a brief description of the moment-based quadrature rule.

The moment equation proposed herein entails evaluating at most  $S$ -dimensional integrals, which is substantially simpler and more efficient than performing one  $N$ -dimensional integration when  $S \ll N$ . For practical problems involving a moderate to large number of input random variables (e.g.  $N > 10$ ), the moment equation presents a promising method. The method does not require calculation of any partial derivatives of response and inversion of random matrices as compared to, respectively, the commonly used Taylor/perturbation and Neumann expansion methods. Hence, the computation effort in conducting probabilistic finite element or meshless analysis is significantly reduced using the dimension-reduction method. The method is coined ' $S$ -variate or multivariate dimension-reduction', since it essentially reduces the calculation of an  $N$ -dimensional integral to that of an at most  $S$ -dimensional integral. When  $S = 1$ , the method degenerates to the univariate dimension-reduction method [20]. When  $S = 2$ , the method becomes the bivariate dimension-reduction method, as described in a previous section of this paper. Similarly, trivariate, quadrivariate, and other higher-variate dimension-reduction methods can be derived by appropriately selecting the value of  $S$ . In the limit, when  $S = N$ , there is no dimension reduction and the proposed method converges to the exact solution.

As described previously, the residual error in the multivariate dimension-reduction method contains terms involving integration of Taylor series with variables of number greater than  $S$ . The error, which decreases as  $S$  increases, can be made arbitrary small if  $S$  is larger and closer to  $N$ . However, more computational effort is required. For example, when evaluating Equation (29) or (32) by an  $n$ -order quadrature rule in each dimension, the total number of function or response evaluations is  $\sum_{i=0}^S \binom{N}{S-i} n^{S-i}$ . In contrast,  $n^N$  function evaluations are required using direct numerical integration without any dimension reduction. Figures 1(a) and (b) show how the ratio  $\sum_{i=0}^S \binom{N}{S-i} n^{S-i} / n^N$  of these two function evaluation numbers varies with respect to  $S$  for  $N = 10$  and 30 when  $n = 3$  and 4, respectively. A reduction of computational effort is achieved when the ratio  $\sum_{i=0}^S \binom{N}{S-i} n^{S-i} / n^N < 1$ . As can be seen in Figures 1(a) and (b) the amount of reduction depends on both  $N$  and  $n$ . For example, univariate, bivariate, and trivariate dimension-reduction methods reduce computational effort by factors of 2000 ( $= \frac{1}{5} \times 10^4$ ), 143 ( $= \frac{1}{7} \times 10^3$ ), and 17 ( $= \frac{1}{6} \times 10^2$ ), respectively, when  $n = 3$  and  $N = 10$ , and by factors of 25 000 ( $= \frac{1}{4} \times 10^5$ ), 1429 ( $= \frac{1}{7} \times 10^4$ ), and 125 ( $= \frac{1}{8} \times 10^3$ ), respectively, when  $n = 4$  and  $N = 10$ . Furthermore, the reduction is dramatically enhanced when  $N$  is larger, as shown in Figures 1(a) and (b).

#### 4.2. Discrete equilibrium equations

Consider a linear mechanical system subject to a vector of input random parameters  $\mathbf{X} \in \mathfrak{R}^N \mapsto (\boldsymbol{\mu}, \boldsymbol{\gamma})$  characterizing uncertainty in the system and loads. Following discretization, let  $\mathbf{Y} \in \mathfrak{R}^M \mapsto (\mathbf{m}_Y, \boldsymbol{\gamma}_Y)$  represent a displacement (response) vector associated with  $M$  degrees of

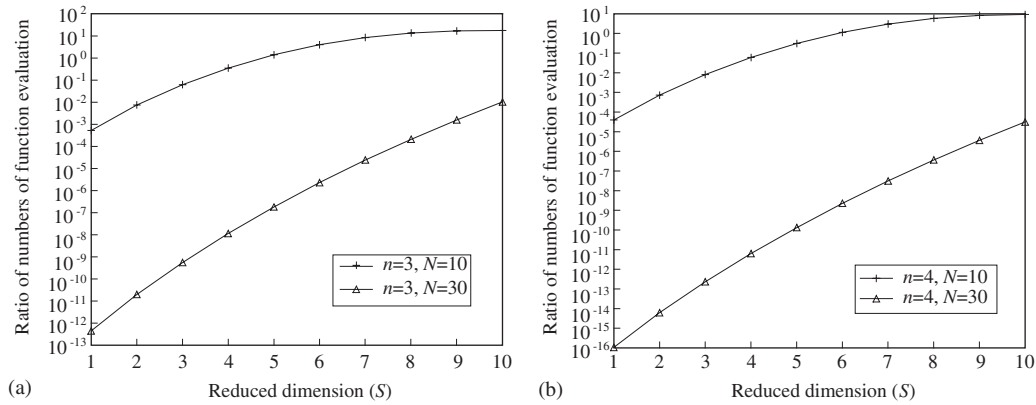


Figure 1. Reduction of computational effort: (a)  $n = 3$ ; and (b)  $n = 4$ .

freedom of the system, satisfying the linear equilibrium equation

$$\mathbf{K}(\mathbf{X})\mathbf{Y}(\mathbf{X}) = \mathbf{F}(\mathbf{X}) \tag{37}$$

in which the stiffness matrix  $\mathbf{K}$  and force vector  $\mathbf{F}$  depend on  $\mathbf{X}$  and represent an elementary stochastic linear operator having random coefficients and involving only algebraic operations. Equation (37) is common to finite-difference, finite-element, and recently developed mesh-free methods when the system, loads, or both, are uncertain. From Equation (37), the solution

$$\mathbf{Y}(\mathbf{X}) = \mathbf{K}(\mathbf{X})^{-1}\mathbf{F}(\mathbf{X}) \tag{38}$$

is random and depends on  $\mathbf{X}$ . Using the multivariate dimension-reduction method, the mean vector  $\mathbf{m}_Y$  and covariance matrix  $\gamma_Y$  of  $\mathbf{Y}$  can be derived as

$$\mathbf{m}_Y = \mathcal{E}[\mathbf{Y}] \cong \mathcal{E}[\hat{\mathbf{Y}}] = \sum_{i=0}^S (-1)^i \binom{N-S+i-1}{i} \sum_{k_1 < k_2 < \dots < k_{S-i}} \mathcal{E}[\mathbf{K}(\tilde{\mathbf{X}}_i)^{-1}\mathbf{F}(\tilde{\mathbf{X}}_i)] \tag{39}$$

$$\gamma_Y = \mathcal{E}[\mathbf{Y}\mathbf{Y}^T] - \mathbf{m}_Y\mathbf{m}_Y^T \tag{40}$$

where  $\tilde{\mathbf{X}}_i = \{0, \dots, 0, X_{k_1}, 0, \dots, 0, X_{k_{S-i}}, 0, \dots, 0\}^T \in \mathfrak{R}^N$  and

$$\mathcal{E}[\mathbf{Y}\mathbf{Y}^T] \cong \sum_{i=0}^S (-1)^i \binom{N-S+i-1}{i} \sum_{k_1 < k_2 < \dots < k_{S-i}} \mathcal{E}[\mathbf{K}(\tilde{\mathbf{X}}_i)^{-1}\mathbf{F}(\tilde{\mathbf{X}}_i)\mathbf{F}(\tilde{\mathbf{X}}_i)^T\mathbf{K}(\tilde{\mathbf{X}}_i)^{-T}] \tag{41}$$

Note that the calculation of expected values on the right-hand side of Equations (39) and (40) involves at most  $S$ -dimensional integrations.

### 5. NUMERICAL EXAMPLES

Two sets of numerical examples are presented to illustrate the proposed multivariate dimension-reduction method. The first set (Examples 1–4) involves elementary mathematical functions and

Table I. Mean of  $Y(\mathbf{X}) = \sqrt{1 + \mathbf{X}^T \mathbf{X}/2}$  by various dimension-reduction methods ( $\sigma = 0.3$ ).

S	N							
	3	4	5	6	7	8	9	10
<i>(a) Dimension-reduction methods</i>								
1	1.065364	1.087152	1.108940	1.130728	1.152516	1.174303	1.196091	1.217879
2	1.064102	1.084629	1.104734	1.124420	1.143684	1.162528	1.180952	1.198955
3	1.064124	1.084716	1.104953	1.124857	1.144449	1.163752	1.182788	1.201578
<i>(b) Numerical integration</i>								
	1.064124	1.084714	1.104944	1.124831	1.144392	1.163641	1.182592	1.201257

the second set (Examples 5–8) involves solid-mechanics problems. The number ( $n$ ) of integration points in each dimension varies from 3 to 4. Whenever possible, comparisons with alternative analytical methods, simulation, and direct numerical integration are provided to evaluate the accuracy, computational efficiency, and convergence of the proposed method.

### 5.1. Example set I—mathematical functions

#### Example 1

Consider an elementary transformation

$$Y(\mathbf{X}) = \sqrt{1 + \mathbf{X}^T \mathbf{X}/2} \quad (42)$$

where  $X_j \mapsto N(0, \sigma^2)$ ,  $j = 1, \dots, N$  are independent and identically distributed Gaussian random variables with mean *zero* and variance  $\sigma^2$ . The multivariate dimension-reduction method was employed to determine the mean of  $Y$  and the relative error, defined as the absolute difference between means obtained by the proposed method and direct numerical integration. Table I shows the mean values of  $Y$  for  $\sigma = 0.3$  and  $N = 3$ –10 using the univariate ( $S = 1$ ), bivariate ( $S = 2$ ), and trivariate ( $S = 3$ ) dimension-reduction methods. A 3rd-order (i.e.  $n = 3$ ) quadrature rule was employed for reduced integration in dimension-reduction methods. Compared with the results of direct  $N$ -dimensional numerical integration, also listed in Table I (last row), the approximate dimension-reduction methods provide satisfactory estimates of mean for all values of  $N$  considered. Furthermore, the approximate means from the dimension-reduction methods converge to the means from direct numerical integration as  $S$  increases.

For larger input uncertainty, Table II presents the relative errors in estimating mean values of  $Y$  when  $\sigma = 1$  and  $N = 3$ –10. The errors, which are listed for various dimension-reduction methods with  $S = 1, 2, 3, 4, 5, 6$ , and 7, consistently decrease with  $S$ . However, the computational effort by dimension-reduction methods increases significantly with  $S$ , as shown in Table III. For example, when  $N = 10$ , the pentavariate ( $S = 5$ ) and heptavariate ( $S = 7$ ) dimension-reduction methods require 81 922 and 497 452 function evaluations to reduce relative errors to 0.003633 and 0.000066, respectively. In contrast, when the same problem is solved using Genz's fully symmetric interpolatory rules [4], 185 085 and 2 779 549 function evaluations are required to reduce relative errors to 0.003741 and 0.000475, respectively. While the function evaluation numbers are very large, it is necessary to point out that the large variation ( $\sigma = 1$ )

Table II. Relative errors by various dimension-reduction methods ( $\sigma = 1.0$ ).

S	N							
	3	4	5	6	7	8	9	10
1	0.033202	0.057051	0.083068	0.110301	0.138172	0.166316	0.194499	0.222567
2	0.002145	0.007381	0.016134	0.028578	0.044751	0.064625	0.088128	0.115170
3	0.000000	0.000448	0.001925	0.005132	0.010748	0.019458	0.031922	0.048783
4		0.000000	0.000101	0.000539	0.001700	0.004117	0.008469	0.015573
5			0.000000	0.000025	0.000157	0.000573	0.001576	0.003633
6				0.000000	0.000006	0.000047	0.000195	0.000600
7					0.000000	0.000002	0.000014	0.000066

Table III. The number of integrand values required by various dimension-reduction methods.

S	N							
	3	4	5	6	7	8	9	10
1	10	13	16	19	22	25	28	31
2	37	67	106	154	211	277	352	436
3	64	175	376	694	1156	1789	2620	3676
4		256	781	1909	3991	7459	12826	20686
5			1024	3367	9094	21067	43444	81922
6				4096	14197	41479	104680	235012
7					16384	58975	183412	497452

case was specifically studied in order to compare dimension-reduction methods with the fully symmetric interpolatory rule, which constitutes one of the most efficient numerical methods known for this problem [4]. For most engineering problems, however, the standard deviation is much smaller; in which case, univariate or bivariate dimension-reduction methods usually suffice in yielding accurate statistical results, as shown in Table I. More realistic examples are presented in the following subsection.

*Example 2*

Let

$$I[y(x_1, \dots, x_N)] \equiv \int_0^1 \dots \int_0^1 \left( \sum_{i=1}^N x_i \right)^{1/2} \prod_{i=1}^N dx_i \tag{43}$$

denote another  $N$ -dimensional integral, for which Entacher [24] developed a quasi-Monte Carlo formula involving a generalized Haar series to determine the integration error. From the reported results in Reference [24], Table IV presents the integration errors for a quasi-Monte Carlo analysis involving 32 768 integrand values. The error measures, which vary from  $4.0 \times 10^{-8}$  to  $3.4 \times 10^{-1}$ , strongly depend on the dimension  $N$  and may differ by orders of magnitude when  $N$  varies from 6 to 9. When using the univariate dimension-reduction method with  $n = 3$ , only 19–28 function evaluations were required to solve this problem, with integration errors on the order of  $10^{-4}$ . The integration errors yielded by the bivariate dimension-reduction method, also shown in Table IV, suggest that errors as low as on the order of  $10^{-5}$  can be achieved

Table IV. Integration errors by quasi-Monte Carlo and dimension-reduction methods.

Dimension ( $N$ )	Integration error		
	Quasi Monte Carlo method (32 768 function evaluations) <sup>†</sup>	Univariate dimension-reduction method (19–28 function evaluations)*	Bivariate dimension-reduction method (154–352 function evaluations) <sup>†</sup>
6	$4.0 \times 10^{-8}$	$3.6 \times 10^{-4}$	$4.1 \times 10^{-5}$
7	$1.5 \times 10^{-5}$	$2.6 \times 10^{-4}$	$2.7 \times 10^{-5}$
8	$1.7 \times 10^{-4}$	$2.0 \times 10^{-4}$	$1.9 \times 10^{-5}$
9	$3.4 \times 10^{-1}$	$1.6 \times 10^{-4}$	$1.3 \times 10^{-5}$

\*Required 19, 22, 25, and 28 integrand values for  $N = 6, 7, 8,$  and  $9,$  respectively.

<sup>†</sup>Required 154, 211, 277 and 352 integrand values for  $N = 6, 7, 8,$  and  $9,$  respectively.

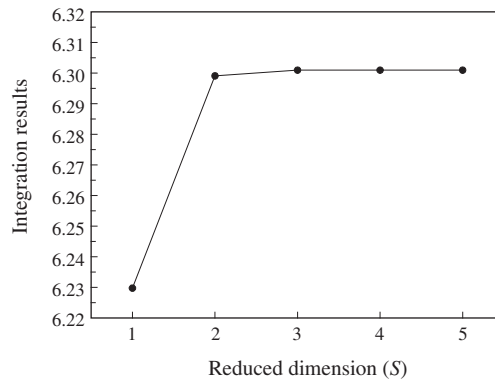


Figure 2. Results of  $\int_0^1 \cdots \int_0^1 \exp(\sum_{i=1}^{10} x_i^2)^{1/2} \prod_{i=1}^{10} dx_i$  by various dimension-reduction methods.

with 154–352 function evaluations, still significantly less than required by the quasi-Monte Carlo method. The dimension-reduction method is not only computationally efficient, but more importantly, yields error estimates that are relatively insensitive to the dimension of the integral.

### Example 3

This 10-dimensional example illustrates the convergence properties of the proposed dimension-reduction method. A multidimensional integral, given by

$$I[y(x_1, \dots, x_{10})] \equiv \int_0^1 \cdots \int_0^1 \exp\left(\sqrt{\sum_{i=1}^{10} x_i^2}\right) \prod_{i=1}^{10} dx_i \quad (44)$$

was evaluated using various dimension-reduction methods with reduced dimension  $S = 1, 2, 3, 4,$  and  $5,$  and the order of integration  $n = 4.$  Figure 2 shows how the integration results vary when  $1 \leq S \leq 5.$  From Figure 2, the proposed method yields a convergent solution as the reduced

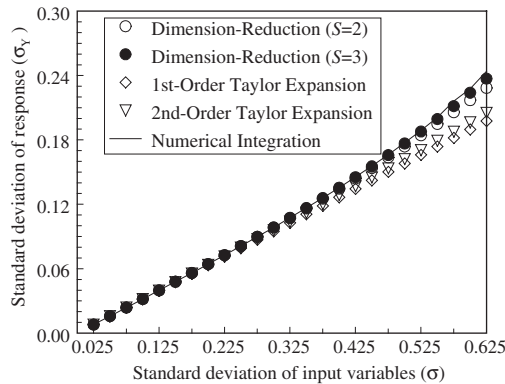


Figure 3. Standard deviations of output  $Y = 1/(1 + \alpha \sum_{j=1}^N X_j)$  for increasing values of input standard deviation.

dimension increases from 1 to 5. The relative difference, i.e. 1.11% between univariate and bivariate dimension-reduction methods and 0.03% between bivariate and trivariate dimension-reduction methods, indicates that univariate or bivariate dimension-reduction methods are often sufficient to generate accurate results.

#### Example 4

The final example in this set entails calculating the standard deviation of the output

$$Y = Y(X_1, \dots, X_N) = \frac{1}{1 + \alpha \sum_{j=1}^N X_j} \quad (45)$$

where input  $X_j \mapsto N(0, \sigma^2)$ ,  $j = 1, \dots, N$  are independent and identically distributed Gaussian random variables. The proposed dimension-reduction method was employed to determine standard deviations  $\sigma_Y$  of  $Y$  for the case  $\alpha = 0.1$  and  $N = 10$ . The results are plotted in Figure 3 for increasing values of input standard deviation. Both bivariate and trivariate dimension-reduction methods provide very good approximations of  $\sigma_Y$ , when compared with the results of direct numerical integration (the reference solution) even for a standard deviation up to 0.625. The comparison with the first- and second-order Taylor expansions, the results of which are also given in Figure 3, suggests that the dimension-reduction methods are superior to the Taylor expansion methods when the standard deviation of input is large, as in this particular problem. Furthermore, the dimension-reduction method can easily generate results of higher accuracy by simply increasing the value of  $S$ . In contrast, it is difficult or impractical to invoke higher-order expansions for Taylor expansion methods, since expensive calculations of higher-order derivatives are required.

#### 5.2. Example set II—solid-mechanics problems

In most of the following solid-mechanics examples, random fields were introduced to increase the dimension of the stochastic problem. For example, lognormal random fields were employed in Examples 5 and 8 to represent the spatial variability of material properties. However, in

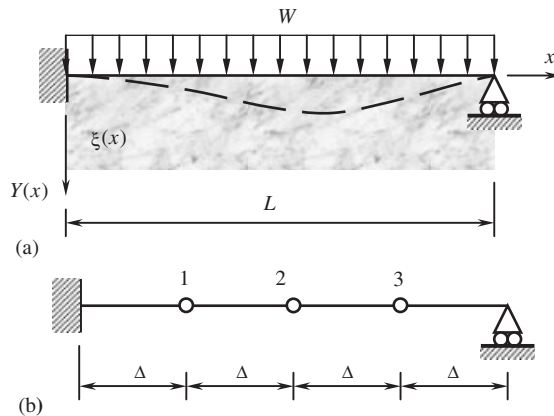


Figure 4. A stochastic beam on an elastic foundation: (a) geometry and loads; and (b) discrete finite-difference model.

Example 6, the elastic modulus was modelled using a Gaussian random field, which although somewhat unrealistic, was adopted here to permit direct comparison of the proposed method with existing methods requiring the Gaussian assumption. The proposed method does not require any specific distribution type of input random variables or fields.

*Example 5 (stochastic finite-difference analysis (linear-elastic))*

Consider a propped cantilever beam on an elastic foundation and its discrete model, as illustrated in Figure 4. For this example, span  $L = 120$  in, nodal spacing  $\Delta = L/4 = 30$  in, and constant beam stiffness  $EI = 6.45 \times 10^8$  lb in<sup>2</sup>. A uniformly distributed load  $W = \exp(V)$  having a lognormal probability distribution with mean  $\mu_W = \exp(\mu_V + \sigma_V^2/2) = 1000$  lb/in, variance  $\sigma_W^2 = \mu_W^2[\exp(\sigma_V^2) - 1]$ , and coefficient of variation  $v_W = \sigma_W/\mu_W$ , where  $\mu_V$  and  $\sigma_V^2$  are mean and variance of normal random variable  $V$ . Finally, the foundation modulus was modelled as a homogeneous lognormal random field  $\xi(x) = \exp[\eta(x)]$  with mean  $\mu_\xi = \exp(\mu_\eta + \sigma_\eta^2/2) = 2000$  lb/in<sup>2</sup>, variance  $\sigma_\xi^2 = \mu_\xi^2[\exp(\sigma_\eta^2) - 1]$ , and coefficient of variation  $v_\xi = \sigma_\xi/\mu_\xi$ , where  $\eta(x)$  is a stationary Gaussian random field with mean  $\mu_\eta$ , variance  $\sigma_\eta^2$ , and covariance function  $\gamma(u) = \mathcal{E}\{[\eta(x+u) - \mu_\eta][\eta(x) - \mu_\eta]\} = \sigma_\eta^2 \exp(-\delta|u|)$ ,  $\delta \geq 0$ . There is no dependence between the applied load and foundation modulus.

The equilibrium equation for the discrete finite-difference model [see Figure 4(b)], including boundary conditions, is

$$\begin{bmatrix} 7 + \zeta X_1 & -4 & 1 \\ -4 & 6 + \zeta X_2 & -4 \\ 1 & -4 & 5 + \zeta X_3 \end{bmatrix} \begin{Bmatrix} Y_1 \\ Y_2 \\ Y_3 \end{Bmatrix} = \begin{Bmatrix} 1 \\ 1 \\ 1 \end{Bmatrix} \zeta X_4 \quad (46)$$

where  $Y_i = Y(i\Delta)$ ,  $i = 1, 2, 3$  is the displacement response at node  $i$ ,  $\zeta = \Delta^4/EI = 1.26 \times 10^{-3}$  in<sup>2</sup>/lb;  $X_j = \xi(j\Delta) = \exp[\eta(j\Delta)]$ ,  $j = 1, 2, 3$ ; and  $X_4 = W = \exp(V)$ . The input lognormal vector  $\mathbf{X} = \{X_1, X_2, X_3, X_4\}^T \in \mathfrak{R}^4$  has mean  $\boldsymbol{\mu} = \{\mu_\xi, \mu_\xi, \mu_\xi, \mu_S\}^T$  and covariance

matrix

$$\gamma = \begin{bmatrix} \sigma_\xi^2 & \sigma_\xi^2 \rho^*(\Delta) & \sigma_\xi^2 \rho^*(2\Delta) & 0 \\ \sigma_\xi^2 \rho^*(\Delta) & \sigma_\xi^2 & \sigma_\xi^2 \rho^*(\Delta) & 0 \\ \sigma_\xi^2 \rho^*(2\Delta) & \sigma_\xi^2 \rho^*(\Delta) & \sigma_\xi^2 & 0 \\ 0 & 0 & 0 & \sigma_S^2 \end{bmatrix} \quad (47)$$

where  $\rho^*(u) = [\exp\{\gamma(u)\} - 1] / [\exp(\sigma_\eta^2) - 1]$ . The objective of this example, originally presented by Grigoriu [18], is to determine the second-moment characteristics of the displacement response  $\mathbf{Y} = \{Y_1, Y_2, Y_3\}^T \in \mathfrak{R}^3$ .

Table V presents the approximate mean and covariance of  $\mathbf{Y}$  for  $\delta\Delta = 0.1$ , obtained using the Monte Carlo simulation (100 000 samples) as well as the results from the univariate dimension-reduction method, bivariate dimension-reduction method, and the statistically equivalent solution [18]. The statistically equivalent solution was developed for stochastic-mechanics problems and was found to be more accurate than first-order Taylor expansion or Neumann expansion methods [18]. The results in Table V are given for three cases of input uncertainties: (a)  $v_\xi = 0.3, v_S = 0.2$ ; (b)  $v_\xi = 0.6, v_S = 0.2$ ; and (c)  $v_\xi = 0.6, v_S = 0.01$ . Simulation results and statistically equivalent solutions were obtained from Reference [18]. In all three cases, the statistically equivalent solution and dimension-reduction method provide almost exact (simulation) estimates of the response mean. However, the dimension-reduction method outperforms the statistically equivalent solution when covariance properties are compared. For example, the ratio of exact to approximate standard deviations lies in the range of (0.81, 1.26) for the statistically equivalent solution, (0.99, 1.04) for the univariate dimension-reduction method and (0.99, 1.01) for the bivariate dimension-reduction method. For each stochastic problem, only 13 and 67 deterministic analyses ( $n = 3$ ) were, respectively, required by the univariate and bivariate dimension-reduction methods.

*Example 6 (stochastic mesh-free analysis (linear-elastic))*

Consider a square plate with a centrally located circular hole, as shown in Figure 5(a). The plate has a dimension of  $2L = 40$  units, a hole with diameter  $2a = 2$  units, and is subjected to a uniformly distributed load of magnitude  $\sigma^\infty = 1$  unit. The Poisson's ratio  $\nu$  was selected to be 0.3. The elastic modulus was assumed to be a homogeneous random field and symmetrically distributed with respect to  $x_1$ - and  $x_2$ -axes [see Figure 5(a)]. The modulus of elasticity  $E(\mathbf{x})$  was represented by  $E(\mathbf{x}) = \mu_E [1 + \alpha(\mathbf{x})]$ , where  $\mu_E = 1$  unit is the constant mean over the domain  $\Omega$ , and  $\alpha(\mathbf{x})$  is a homogeneous Gaussian random field with mean *zero* and covariance function

$$\Gamma_\alpha(\xi) = \mathcal{E}[\alpha(\mathbf{x})\alpha(\mathbf{x} + \xi)] = \sigma_\alpha^2 \exp\left[-\frac{\|\xi\|}{bL}\right], \quad \forall \mathbf{x}, \mathbf{x} + \xi \in \Omega \quad (48)$$

where  $\sigma_\alpha = 0.1$  unit and  $b = 0.5$ . Due to symmetry, only a quarter of the plate, represented by the region ABEDC and shaded in Figure 5(a), was analysed. Figure 5(b) presents a meshless discretization of the quarter plate with 90 nodes [8, 15].

The random field  $\alpha(\mathbf{x})$  was parameterized using the Karhunen–Loève expansion [35]

$$\alpha(\mathbf{x}) \cong \sum_{j=1}^N X_j \sqrt{\lambda_j} \phi_j(\mathbf{x}) \quad (49)$$

Table V. Mean and covariance of displacement vector  $\mathbf{Y}$  in beam on elastic foundation for  $\delta\Delta = 0.1$ .

	Statistically equivalent solution [18]	Univariate dimension-reduction method	Bivariate dimension-reduction method	Monte Carlo simulation [18] ( $10^5$ samples)
(a) $v_z = 0.3$ ; $v_S = 0.2$				
Mean vector ( $\mathbf{m}_Y$ )	$\begin{Bmatrix} 0.295 \\ 0.480 \\ 0.391 \end{Bmatrix}$	$\begin{Bmatrix} 0.297 \\ 0.480 \\ 0.391 \end{Bmatrix}$	$\begin{Bmatrix} 0.297 \\ 0.480 \\ 0.392 \end{Bmatrix}$	$\begin{Bmatrix} 0.297 \\ 0.480 \\ 0.392 \end{Bmatrix}$
Covariance matrix ( $\gamma_Y$ )	$\begin{bmatrix} 0.0044 & 0.0085 & 0.0067 \\ 0.0168 & 0.0133 & 0.0159 \\ 0.0107 & 0.0130 & 0.0138 \end{bmatrix}$	$\begin{bmatrix} 0.0066 & 0.0113 & 0.0091 \\ 0.0198 & 0.0159 & 0.0170 \\ 0.0130 & 0.0138 & 0.0138 \end{bmatrix}$ (sym.)	$\begin{bmatrix} 0.0070 & 0.0120 & 0.0096 \\ 0.0211 & 0.0170 & 0.0170 \\ 0.0138 & 0.0138 & 0.0138 \end{bmatrix}$ (sym.)	$\begin{bmatrix} 0.0070 & 0.0121 & 0.0096 \\ 0.0212 & 0.0170 & 0.0170 \\ 0.0139 & 0.0139 & 0.0139 \end{bmatrix}$ (sym.)
(b) $v_z = 0.6$ ; $v_S = 0.2$				
Mean vector ( $\mathbf{m}_Y$ )	$\begin{Bmatrix} 0.328 \\ 0.540 \\ 0.441 \end{Bmatrix}$	$\begin{Bmatrix} 0.328 \\ 0.540 \\ 0.439 \end{Bmatrix}$	$\begin{Bmatrix} 0.328 \\ 0.540 \\ 0.439 \end{Bmatrix}$	$\begin{Bmatrix} 0.328 \\ 0.539 \\ 0.439 \end{Bmatrix}$
Covariance matrix ( $\gamma_Y$ )	$\begin{bmatrix} 0.0205 & 0.0388 & 0.0307 \\ 0.0746 & 0.0595 & 0.0428 \\ 0.0480 & 0.0480 & 0.0348 \end{bmatrix}$ (sym.)	$\begin{bmatrix} 0.0163 & 0.0292 & 0.0231 \\ 0.0535 & 0.0428 & 0.0348 \\ 0.0348 & 0.0348 & 0.0348 \end{bmatrix}$ (sym.)	$\begin{bmatrix} 0.0175 & 0.0316 & 0.0250 \\ 0.0581 & 0.0465 & 0.0377 \\ 0.0377 & 0.0377 & 0.0377 \end{bmatrix}$ (sym.)	$\begin{bmatrix} 0.0173 & 0.0312 & 0.0247 \\ 0.0573 & 0.0459 & 0.0373 \\ 0.0373 & 0.0373 & 0.0373 \end{bmatrix}$ (sym.)
(c) $v_z = 0.6$ ; $v_S = 0.01$				
Mean vector ( $\mathbf{m}_Y$ )	$\begin{Bmatrix} 0.327 \\ 0.540 \\ 0.441 \end{Bmatrix}$	$\begin{Bmatrix} 0.328 \\ 0.540 \\ 0.440 \end{Bmatrix}$	$\begin{Bmatrix} 0.328 \\ 0.540 \\ 0.440 \end{Bmatrix}$	$\begin{Bmatrix} 0.328 \\ 0.540 \\ 0.439 \end{Bmatrix}$
Covariance matrix ( $\gamma_Y$ )	$\begin{bmatrix} 0.0188 & 0.0353 & 0.0279 \\ 0.0669 & 0.0534 & 0.0360 \\ 0.0432 & 0.0432 & 0.0293 \end{bmatrix}$ (sym.)	$\begin{bmatrix} 0.0129 & 0.0238 & 0.0187 \\ 0.0451 & 0.0360 & 0.0293 \\ 0.0293 & 0.0293 & 0.0293 \end{bmatrix}$ (sym.)	$\begin{bmatrix} 0.0127 & 0.0235 & 0.0185 \\ 0.0446 & 0.0355 & 0.0288 \\ 0.0288 & 0.0288 & 0.0288 \end{bmatrix}$ (sym.)	$\begin{bmatrix} 0.0126 & 0.0233 & 0.0184 \\ 0.0442 & 0.0352 & 0.0285 \\ 0.0285 & 0.0285 & 0.0285 \end{bmatrix}$ (sym.)

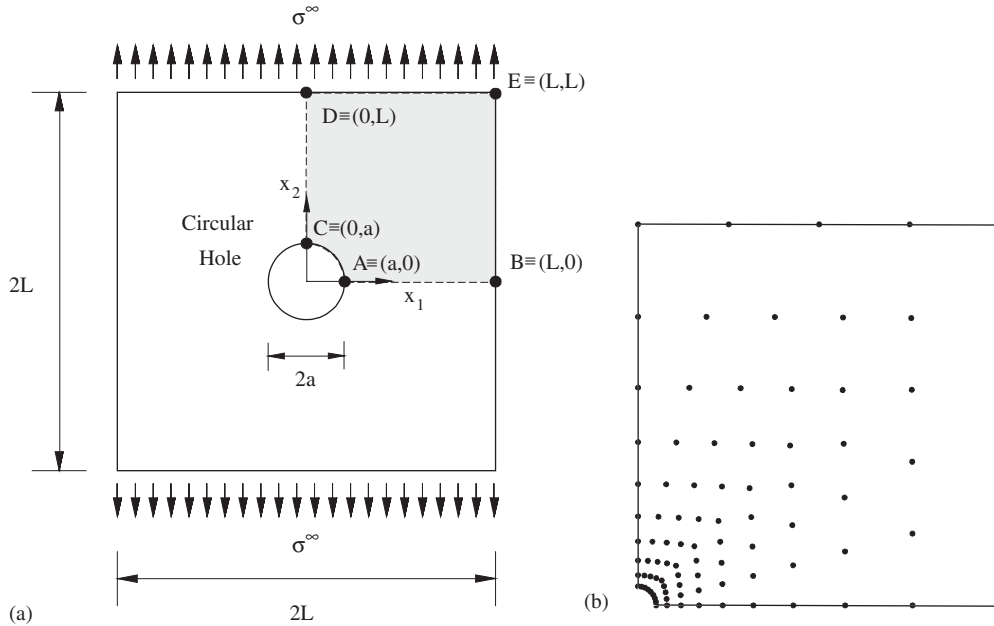


Figure 5. A square plate with a hole subjected to uniformly distributed tension: (a) geometry and loads; and (b) meshless discretization.

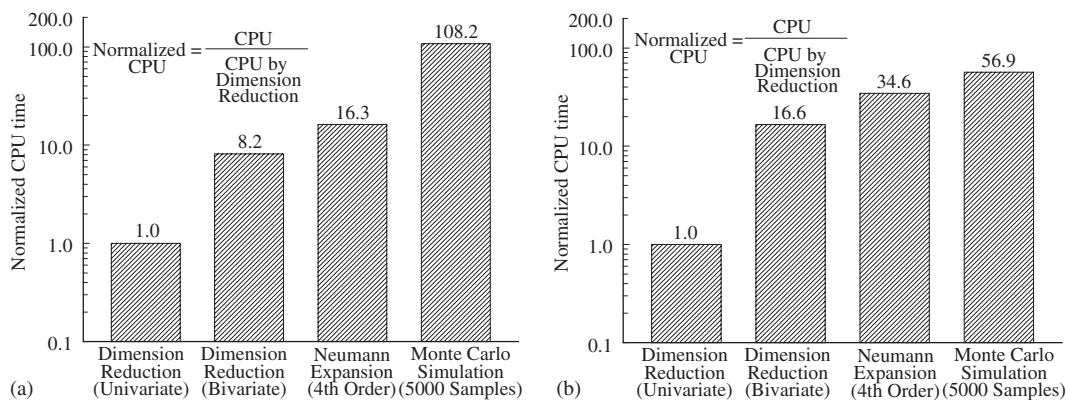
where  $X_j \mapsto N(0, 1)$ ,  $j = 1, \dots, N$  are standard and independent Gaussian random variables and  $\{\lambda_j, \phi_j(\mathbf{x})\}$ ,  $j = 1, \dots, N$  are the eigenvalues and eigenfunctions, respectively, of the covariance kernel. Mesh-free shape functions were employed to solve the associated integral equation needed to calculate the eigenvalues and eigenfunctions [15]. Based on the correlation parameter  $b = 0.5$ , a value of  $N = 12$  was selected to adequately represent  $\alpha(\mathbf{x})$ . Based on the Karhunen–Loève discretization, the input uncertainty was represented by a 12-dimensional standard Gaussian vector  $\mathbf{X} \mapsto N(\mathbf{0}, \mathbf{I})$ , where  $\mathbf{0} \in \mathfrak{R}^{12}$  and  $\mathbf{I} \in \mathcal{L}(\mathfrak{R}^{12} \times \mathfrak{R}^{12})$  are the null vector and identity matrix, respectively.

Table VI presents standard deviations of displacements and strains at points  $A, B, C, D$ , and  $E$  [see Figure 5(a)], predicted by the proposed dimension-reduction method (Equations (39)–(41)), as well as results of a fourth-order Neumann expansion method and a Monte Carlo simulation (5000 samples). The Neumann expansion solutions were obtained following the development by Ghanem and Spanos [14]. As can be seen in Table VI, the Neumann expansion and dimension-reduction methods provide satisfactory results for prediction of standard deviations in comparison with simulation results. The accuracy of the response statistics from the bivariate dimension-reduction method is slightly higher than Neumann expansion and univariate dimension-reduction methods. More importantly, however, a comparison of CPU times, obtained for two separate analyses for  $N = 6$  and 12 as shown in Figures 6(a) and (b), respectively, indicates that the univariate dimension-reduction method is far more efficient than the Neumann expansion method. From Table VI and Figures 6(a) and (b), it can be seen that the bivariate dimension-reduction method surpasses both the accuracy (marginally) and computational efficiency of the fourth-order Neumann expansion method.

Table VI. Standard deviations of displacement and strains in plate with a hole by various methods ( $N = 12$ ).

Location	Response variable*	Standard deviation of response			
		4th-Order Neumann expansion method	Univariate dimension-reduction method	Bivariate dimension-reduction method	Monte Carlo simulation (5000 samples)
A	$u_1$	$1.11 \times 10^{-1}$	$1.09 \times 10^{-1}$	$1.12 \times 10^{-1}$	$1.12 \times 10^{-1}$
	$\varepsilon_{11}$	$2.58 \times 10^{-2}$	$2.53 \times 10^{-2}$	$2.58 \times 10^{-2}$	$2.56 \times 10^{-2}$
	$\varepsilon_{22}$	$2.39 \times 10^{-1}$	$2.34 \times 10^{-1}$	$2.39 \times 10^{-1}$	$2.37 \times 10^{-1}$
	$\varepsilon_{12}$	$3.28 \times 10^{-2}$	$3.22 \times 10^{-2}$	$3.28 \times 10^{-2}$	$3.25 \times 10^{-2}$
B	$u_1$	$4.60 \times 10^{-1}$	$4.52 \times 10^{-1}$	$4.61 \times 10^{-1}$	$4.61 \times 10^{-1}$
	$\varepsilon_{22}$	$7.97 \times 10^{-2}$	$7.82 \times 10^{-2}$	$7.97 \times 10^{-2}$	$8.21 \times 10^{-2}$
C	$u_2$	$2.48 \times 10^{-1}$	$2.43 \times 10^{-1}$	$2.49 \times 10^{-1}$	$2.46 \times 10^{-1}$
	$\varepsilon_{11}$	$8.64 \times 10^{-2}$	$8.48 \times 10^{-2}$	$8.65 \times 10^{-2}$	$8.72 \times 10^{-2}$
	$\varepsilon_{22}$	$1.28 \times 10^{-2}$	$1.26 \times 10^{-2}$	$1.28 \times 10^{-2}$	$1.28 \times 10^{-2}$
	$\varepsilon_{12}$	$3.89 \times 10^{-2}$	$3.81 \times 10^{-2}$	$3.89 \times 10^{-2}$	$3.90 \times 10^{-2}$
D	$u_2$	1.33	1.30	1.33	1.33
	$\varepsilon_{22}$	$8.30 \times 10^{-2}$	$8.10 \times 10^{-2}$	$8.31 \times 10^{-2}$	$8.34 \times 10^{-2}$
E	$u_1$	$5.94 \times 10^{-1}$	$5.83 \times 10^{-1}$	$5.95 \times 10^{-1}$	$5.99 \times 10^{-1}$
	$u_2$	1.37	1.35	1.37	1.38
	$\varepsilon_{22}$	$8.36 \times 10^{-2}$	$8.17 \times 10^{-2}$	$8.37 \times 10^{-2}$	$8.37 \times 10^{-2}$

\* $u_1$  and  $u_2$  are horizontal and vertical displacements, respectively.  $\varepsilon_{11}$  and  $\varepsilon_{22}$  represent normal tensorial strains in  $x_1$  and  $x_2$  directions, respectively; and  $\varepsilon_{12}$  represents tensorial shear strain.

Figure 6. Comparison of CPU time by various methods: (a)  $N = 6$ ; and (b)  $N = 12$ .

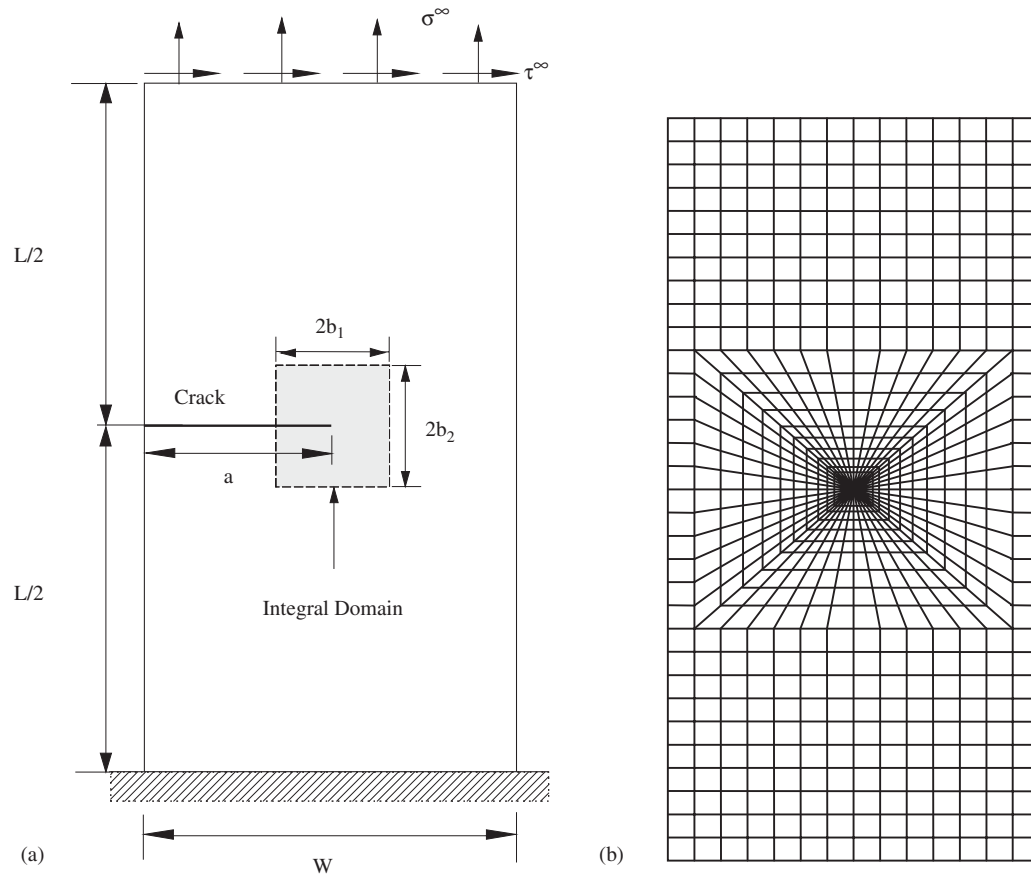


Figure 7. Edge-cracked plate subject to mixed-mode loading conditions: (a) geometry and loads; and (b) finite-element discretization.

*Example 7 (stochastic finite element analysis (linear-elastic))*

A homogeneous, edge-cracked plate is presented to illustrate a mixed-mode probabilistic fracture-mechanics analysis using the dimension-reduction method. As shown in Figure 7(a), a plate of length  $L = 16$  units was fixed at the bottom and subjected to a far-field normal stress  $\sigma^\infty$  and a shear stress  $\tau^\infty$  applied at the top. The plate was analysed using the finite element method involving a total of 832 8-noded quadrilateral elements and 48 quarter-point triangular elements at the crack-tip, as shown in Figure 7(b). The independent random variables are: (1) uniformly distributed crack length  $a \mapsto U(2.8, 4.2)$  units; (2) uniformly distributed plate width  $W \mapsto U(7, 8)$ ; (3) Gaussian normal stress  $\sigma^\infty \mapsto N(1, 0.1^2)$ ; and (4) Gaussian shear stress  $\tau^\infty \mapsto N(1, 0.1^2)$ . The elastic modulus and Poisson's ratio were  $30 \times 10^6$  units and 0.25, respectively. A plane strain condition was assumed.

Table VII presents the predicted means and standard deviations of stress-intensity factors  $K_I$  and  $K_{II}$  obtained using the proposed univariate and bivariate dimension-reduction methods

Table VII. Means and standard deviations of mixed-mode fracture parameters.

Response and computational effort	Univariate dimension-reduction method		Bivariate dimension-reduction method		Numerical integration	
	Mean	Standard deviation	Mean	Standard deviation	Mean	Standard deviation
$K_I$	39.302	7.828	39.328	8.081	39.328	8.083
$K_{II}$	4.411	0.737	4.411	0.741	4.411	0.741
No. of analyses		13		67		81

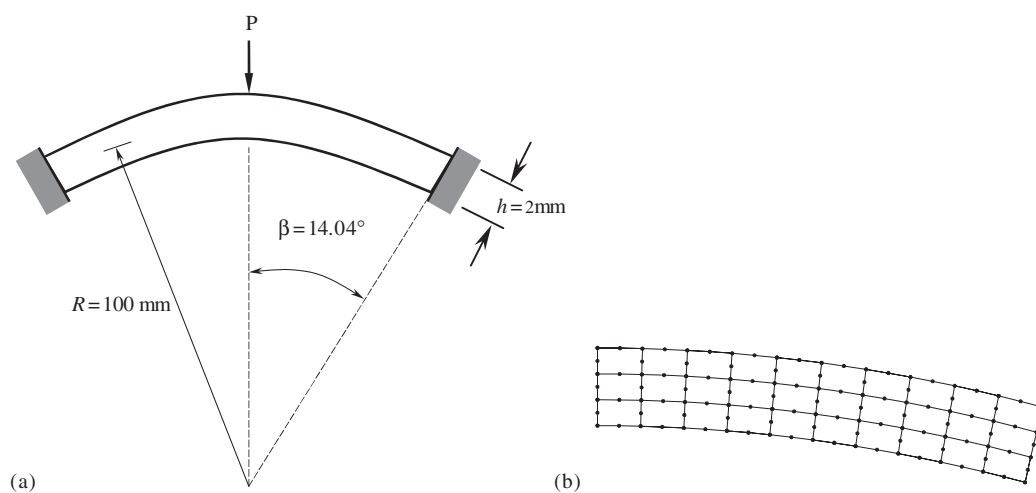


Figure 8. A shallow arch subject to concentrated load: (a) geometry and loads; and (b) finite-element discretization.

as well as results obtained from numerical integration. The results in Table VII clearly show that the dimension-reduction methods can accurately calculate the statistical characteristics of fracture parameters. Only 13 and 67 finite element analyses, respectively, were needed by the univariate and bivariate dimension-reduction methods.

#### Example 8 (Stochastic finite element analysis (non-linear, large-deformation))

In this final example, the proposed dimension-reduction method was employed to solve a non-linear problem in solid-mechanics. Figure 8(a) illustrates a shallow circular arch, with mean radius  $R = 100$  mm, rectangular cross-section with depth  $h = 2$  mm, thickness  $t = 1$  mm, and arc angle  $2\beta = 28.1^\circ$ . The arch, fixed at both ends, was subjected to a concentrated load  $P = 200$  N at the centre. The Poisson's ratio was zero in this example. A finite element mesh employing 30 8-noded quadrilateral elements was used to model the arch, as shown in Figure 8(b). The stress analysis involved large-deformation behaviour for modelling the geometric non-linearity of the arch. A plane stress condition was assumed.

Table VIII. Statistical moments of central deflection of shallow arch by various methods.

Statistical moments ( $m_l = \mathcal{E}[Y^l]$ )	1st-order Taylor expansion method	2nd-order Taylor expansion method	Univariate dimension-reduction method	Bivariate dimension-reduction method	Numerical integration
(a) Case 1: $\sigma_E = 8 \text{ kN/mm}^2$					
$m_1$	1.6410	1.7192	1.7491	1.7423	1.7413
$m_2$	2.7641	3.0573	3.1929	3.1808	3.1735
$m_3$	4.7699	5.6679	6.1191	6.1348	6.1035
$m_4$	8.4187	11.055	12.382	12.584	12.478
$m_5$	15.176	22.908	26.567	27.533	27.229
(b) Case 2: $\sigma_E = 16 \text{ kN/mm}^2$					
$m_1$	1.7441	2.2288	2.1947	2.0129	2.0402
$m_2$	3.4769	6.5935	5.3093	4.6199	4.7406
$m_3$	7.5815	27.000	13.659	11.9604	12.333
$m_4$	17.761	151.94	36.576	33.9896	34.904
$m_5$	44.169	1112.7	101.08	102.920	104.581
(c) Case 3: $\sigma_E = 24 \text{ kN/mm}^2$					
$m_1$	1.9794	4.8551	2.3132	2.2093	2.2221
$m_2$	6.5648	69.478	6.4170	5.6938	5.7778
$m_3$	23.472	1531.9	19.967	16.646	17.009
$m_4$	98.585	49219	66.074	53.260	54.574
$m_5$	443.63	2016819	225.80	180.77	185.07

The modulus of elasticity  $E(\mathbf{x})$  was represented by a homogeneous, lognormal translation field  $E(\mathbf{x}) = c_\alpha \exp[\alpha(\mathbf{x})]$ , of mean  $\mu_E = 80 \text{ kN/mm}^2$  and standard deviation  $\sigma_E$  for which  $\alpha(\mathbf{x})$  is a zero-mean, homogeneous, Gaussian random field with standard deviation  $\sigma_\alpha = \sqrt{\ln(1 + \sigma_E^2/\mu_E^2)}$ , an exponential covariance function represented by Equation (48),  $b = 0.1$ ; and  $c_\alpha = \mu_E \exp(-\sigma_\alpha^2/2) = \mu_E^2/\sqrt{\mu_E^2 + \sigma_E^2}$ . The Karhunen–Loève expansion was employed to discretize the random field  $\alpha(\mathbf{x})$  into four-standard Gaussian random variables.

Due to uncertainty in the elastic modulus, any mechanical response of this arch is stochastic. Table VIII presents estimates of the first five moments  $m_l = \mathcal{E}[Y^l]$ ,  $l = 1, \dots, 5$  of the deflection  $Y$  at the central point of the arch, obtained using the first- and second-order Taylor expansion methods, the univariate dimension-reduction method, and the bivariate dimension-reduction method. The gradients required in the Taylor expansion were obtained using standard finite-difference equations. To evaluate the approximate methods, direct, four-dimensional numerical integrations were also performed to generate benchmark solutions. The results in Table VIII pertain to three cases of statistical input: (a)  $\sigma_E = 8 \text{ kN/mm}^2$ ; (b)  $\sigma_E = 16 \text{ kN/mm}^2$ ; and (c)  $\sigma_E = 24 \text{ kN/mm}^2$ , representing small, moderate, and large uncertainties of elastic modulus. A deterministic load  $P = 200 \text{ N}$  was applied since the arch demonstrates the largest instability in the vicinity of this load [20]. The results presented in Table VIII indicate that the univariate and bivariate dimension-reduction methods provide excellent estimates of statistical moments for all three cases of input. For a given problem (case), the proposed univariate and bivariate

dimension-reduction methods, respectively, required only 17 and 113 analyses ( $n = 4$ ), as opposed to  $4^4 = 256$  analyses using numerical integration. The first- and second-order Taylor expansion methods also yield good estimates of response moments, but only for the first case when input uncertainties are small. However, for moderate uncertainties of input (second case), the Taylor expansion methods are able to predict only lower-order moments, such as first and second moments, reasonably fairly, but the statistical accuracy rapidly degrades when estimating higher-order moments. In the third case, when input uncertainties are large, the first-order Taylor expansion method slightly underestimates the mean response, but grossly overestimates higher-order moments. For the same case, due to large second-order gradients, the second-order Taylor expansion method significantly overpredicts all statistical moments of response, thus failing to generate acceptable results. In contrast, the dimension-reduction methods provide excellent estimates of higher-order moments even for large variation of input, and therefore, should provide a better approximation of the tail of the response distribution than the Taylor expansion methods.

## 6. CONCLUSIONS

A new, generalized, multivariate dimension-reduction method was developed for calculating statistical moments of response of mechanical systems subject to uncertainties in loads, material properties, and geometry. The method involves an additive decomposition of an  $N$ -dimensional response function into at most  $S$ -dimensional functions, where  $S \ll N$ , an approximation of response moments by moments of input random variables; and a moment-based quadrature rule for numerical integration. A new theorem is presented, which provides a convenient means to represent the Taylor series up to a specific dimension without the need for any partial derivatives. A complete proof of the theorem has been presented using two lemmas, also proved in this paper. Unlike commonly used Taylor expansion/perturbation methods and Neumann expansion method, the proposed method respectively requires neither the calculation of partial derivatives of response nor the inversion of random matrices. Eight numerical examples involving elementary mathematical functions and solid-mechanics problems have been presented to illustrate the benefits of the proposed method. Results indicate that the multivariate dimension-reduction method generates convergent solutions and provides more accurate estimates of statistical moments or multidimensional integration than existing methods, such as first- and second-order Taylor expansion methods, statistically equivalent solutions, quasi-Monte Carlo simulation, and fully symmetric interpolatory rule. While the accuracy of the dimension-reduction method is comparable to that of the fourth-order Neumann expansion method, a comparison of CPU time suggests that the former is computationally far more efficient than the latter.

## APPENDIX A: MOMENT-BASED QUADRATURE RULE

Consider a transformation  $\tilde{\mathbf{X}} = \tilde{\mathbf{X}}(\mathbf{U})$  that involves mapping a dependent random vector  $\tilde{\mathbf{X}} \in \mathfrak{R}^I$  to an independent random vector  $\mathbf{U} = \{U_1, \dots, U_I\}^T \in \mathfrak{R}^I$ , where  $I = S - i$ . If  $f_{U_i}(u_i)$  represents the probability density function of  $U_j$ ,  $j = 1, \dots, I$ , Equation (33) becomes

$$\begin{aligned} & \mathcal{E}[Z(0, \dots, 0, X_{k_1}, 0, \dots, 0, X_{k_2}, 0, \dots, 0, X_{k_I}, 0, \dots, 0)] \\ & = \mathcal{E}[\tilde{Z}(U_1, \dots, U_I)] \end{aligned}$$

$$\begin{aligned}
 &= \int_{-\infty}^{\infty} \bar{z}(u_1, \dots, u_I) f_{U_1}(u_1) \cdots f_{U_I}(u_I) \mathbf{d}\mathbf{u} \\
 &\cong \sum_{i_1=1}^n \cdots \sum_{i_I=1}^n \prod_{j=1}^I w_{j,i_j} \bar{z}(u_{1,i_1}, \dots, u_{I,i_I})
 \end{aligned} \tag{A1}$$

where  $\bar{Z}(U_1, \dots, U_I)$  is the transformed function,  $u_{j,i}$ ,  $i = 1, \dots, n$  and  $w_{j,i}$  are the integration point and associated weight, respectively, for the  $u_j$  co-ordinate selected using the moment-based quadrature rule [20], as follows.

To construct a moment-based integration rule with  $n$  interpolation points  $u_{j,i}$ ,  $i = 1, \dots, n$  in the direction of the  $u_j$  co-ordinate, define a function

$$P(u_j) = \prod_{i=1}^n (u_j - u_{j,i}) f_{U_j}(u_j) \tag{A2}$$

which satisfies

$$\int_{-\infty}^{\infty} P(u_j)(u_j)^i \mathbf{d}u_j = 0; \quad i = 0, 1, \dots, n - 1 \tag{A3}$$

If

$$r_{j,k} = \sum_{i_1=1}^n \sum_{i_2=1, \neq i_1}^n \cdots \sum_{i_k=1, \neq i_1, i_2, \dots, i_{k-1}}^n u_{j,i_1} u_{j,i_2} \cdots u_{j,i_k}; \quad k = 1, \dots, n \tag{A4}$$

Equation (A3) yields a system of linear equations

$$\begin{bmatrix}
 \mu_{j,n-1} & -\mu_{j,n-2} & \mu_{j,n-3} & \cdots & (-1)^{n-1} \mu_{j,0} \\
 \mu_{j,n} & -\mu_{j,n-1} & \mu_{j,n-2} & \cdots & (-1)^{n-1} \mu_{j,1} \\
 \mu_{j,n+1} & -\mu_{j,n} & \mu_{j,n-1} & \cdots & (-1)^{n-1} \mu_{j,2} \\
 \vdots & \vdots & \vdots & & \vdots \\
 \mu_{j,2n-2} & -\mu_{j,2n-3} & \mu_{j,2n-4} & \cdots & (-1)^{n-1} \mu_{j,n-1}
 \end{bmatrix}
 \begin{bmatrix}
 r_{j,1} \\
 r_{j,2} \\
 r_{j,3} \\
 \vdots \\
 r_{j,n}
 \end{bmatrix}
 =
 \begin{bmatrix}
 \mu_{j,n} \\
 \mu_{j,n+1} \\
 \mu_{j,n+2} \\
 \vdots \\
 \mu_{j,2n-1}
 \end{bmatrix} \tag{A5}$$

where the coefficient matrix consists of known moments of random variable  $U_j$ , given by

$$\mu_{j,i} = \int_{-\infty}^{\infty} (u_j)^i f_{U_j}(u_j) \mathbf{d}u_j \tag{A6}$$

After solving  $r_{j,i}$  from Equation (A5),  $u_{j,i}$ ,  $i = 1, \dots, n$  can be obtained as the  $i$ th root of

$$u_j^n - r_{j,1} u_j^{n-1} + r_{j,2} u_j^{n-2} - \cdots + (-1)^n r_{j,n} = 0 \tag{A7}$$

For a shape function defined as

$$\phi_{j,i}^{(n-1)}(t_j) \cong \frac{f_{U_j}(u_j) \prod_{k=1, k \neq i}^n (u_j - u_{j,k})}{f_{U_j}(u_{j,i}) \prod_{k=1, k \neq i}^n (u_{j,i} - u_{j,k})} \tag{A8}$$

it can be shown by polynomial approximation that

$$\begin{aligned} & \bar{z}(u_1, \dots, u_I) f_{U_j}(u_j) \\ & \cong \sum_{i=1}^n \phi_{j,i}^{(n-1)}(t_j) \bar{z}(u_1, \dots, u_{j,i}, u_{j+1}, \dots, u_I) f_{U_j}(u_{j,i}) + \sum_{i=0}^{n-1} \beta_{j,i} (u_j)^i P(u_j) \end{aligned} \quad (\text{A9})$$

where  $\beta_{j,i} \in (-\infty, \infty)$ ,  $i = 0, n-1$  are constants. Hence, Equations (A3) and (A9) yield

$$\int_{-\infty}^{\infty} \bar{z}(u_1, \dots, u_I) f_{U_j}(u_j) du_j \cong \sum_{i=1}^n w_{j,i} \bar{z}(u_1, \dots, u_{j,i}, u_{j+1}, \dots, u_I) \quad (\text{A10})$$

where

$$w_{j,i} = \frac{\int_{-\infty}^{\infty} \prod_{k=1, k \neq i}^n (u_j - u_{j,k}) f_{U_j}(u_j) du_j}{\prod_{k=1, k \neq i}^n (u_{j,i} - u_{j,k})} = \frac{\sum_{k=0}^{n-1} (-1)^k \mu_{j,n-k-1} q_{j,ik}}{\prod_{k=1, k \neq i}^n (u_{j,i} - u_{j,k})} \quad (\text{A11})$$

is the  $i$ th weight for the  $j$ th variable  $U_j$ , which is consistent with its moments,  $q_{j,i0} = 1$ , and  $q_{j,ik} = r_{j,k} - u_{j,i} q_{j,i(k-1)}$ . It should be noted that Equation (A7) generates integration points and Equation (A11) yields the weights of Gauss–Legendre or Gauss–Hermite quadratures [34] when the random variable  $U_j$  follows uniform or Gaussian probability distributions, respectively.

#### ACKNOWLEDGEMENTS

The authors would like to acknowledge the financial support from the U.S. National Science Foundation (CMS-9733058, CMS-9900196 and DMI-0355487) and the U.S. Army sponsored Automotive Research Centre.

#### REFERENCES

1. Grigoriu M. *Stochastic Calculus—Applications in Science and Engineering*. Birkhäuser, Springer: New York, NY, 2002.
2. Madsen HO, Krenk S, Lind NC. *Methods of Structural Safety*. Prentice-Hall, Inc.: Englewood Cliffs, NJ, 1986.
3. IASSAR Subcommittee on Computational stochastic Structural Mechanics. A state-of-the-art report on computational stochastic mechanics. *Probabilistic Engineering Mechanics* 1997; **12**(4):197–321.
4. Genz AC, Keister BD. Fully symmetric interpolatory rules for multiple integrals over infinite regions with Gaussian weight. *Journal of Computational and Applied Mathematics* 1996; **71**:299–309.
5. Genz AC, Monahan J. A stochastic algorithm for high-dimensional integrals over unbounded regions with Gaussian weight. *Journal of Computational and Applied Mathematics* 1999; **112**:71–81.
6. Genz AC, Malik AA. An imbedded family of fully symmetric numerical integration rules. *SIAM Journal on Numerical Analysis* 1983; **20**:580–588.
7. Kleiber M, Hien TD. *The Stochastic Finite Element Method*. Wiley: New York, NY, 1992.
8. Rahman S, Rao BN. A perturbation method for stochastic meshless analysis in elastostatics. *International Journal for Numerical Methods in Engineering* 2001; **50**:1969–1991.
9. Liu WK, Belytschko T, Mani A. Random field finite elements. *International Journal for Numerical Methods in Engineering* 1986; **23**:1831–1845.
10. Shinozuka M, Astill J. Random eigenvalue problems in structural mechanics. *AIAA Journal* 1972; **10**:456–462.
11. Adomian G, Malakian K. Inversion of stochastic partial differential operators—the linear case. *Journal of Mathematical Analysis and Applications* 1980; **77**:505–512.

12. Yamazaki F, Shinozuka M. Neumann expansion for stochastic finite element analysis. *Journal of Engineering Mechanics* (ASCE) 1988; **114**:1335–1354.
13. Spanos PD, Ghanem RG. Stochastic finite element expansion for random media. *Journal of Engineering Mechanics* (ASCE) 1989; **115**:1035–1053.
14. Ghanem RG, Spanos PD. *Stochastic Finite Elements: A Spectral Approach*. Springer: New York, NY, 1991.
15. Rahman S, Xu H. A meshless method for computational stochastic mechanics. *International Journal of Computational Engineering Science*, 2004, in press.
16. Adomian G. *Applied Stochastic Processes*. Academic Press: New York, NY, 1980.
17. Adomian G. *Stochastic Systems*. Academic Press: New York, NY, 1980.
18. Grigoriu M. Statistically equivalent solutions of stochastic mechanics problems. *Journal of Engineering Mechanics* (ASCE) 1991; **117**:1906–1918.
19. Rosenblueth E. Two-point estimates in probabilities. *Applied Mathematical Modelling* 1981; **5**:329–335.
20. Rahman S, Xu H. A univariate dimension-reduction method for multi-dimensional integration in stochastic mechanics. *Probabilistic Engineering Mechanics*, 2004, in press.
21. Rubinstein RY. *Simulation and the Monte Carlo Method*. Wiley: New York, 1981.
22. Niederreiter H, Spanier J. *Monte Carlo and Quasi-Monte Carlo Methods*. Springer: Berlin, 2000.
23. Sobol IM. On Quasi-Monte Carlo integrations. *Mathematics and Computers in Simulation* 1998; **47**:103–112.
24. Entacher K. Quasi-Monte Carlo methods for numerical integration of multivariate Haar Series. *BIT* 1997; **4**(37):845–860.
25. Englund S, Rackwitz R. A benchmark study on importance sampling techniques in structural reliability. *Structural Safety* 1993; **12**:255–276.
26. Melchers RE. Importance sampling in structural systems. *Structural Safety* 1989; **6**:3–10.
27. Bjerager P. Probability integration by directional simulation. *Journal of Engineering Mechanics* (ASCE) 1988; **114**:1285–1302.
28. Nie J, Ellingwood BR. Directional methods for structural reliability analysis. *Structural Safety* 2000; **22**: 233–249.
29. McKay MD, Conover WJ, Beckman RJ. A comparison of three methods for selecting values of input variables in the analysis of output from a computer code. *Technometrics* 1979; **21**:239–245.
30. Stein M. Large sample properties of simulations using latin hypercube sampling. *Technometrics* 1987; **29**:143–150.
31. Gilks WR, Richardson S, Spiegelhalter DJ. *Markov Chain Monte Carlo in Practice*. Chapman & Hall: London, 1996.
32. Nelson BL. Decomposition of some well-known variance reduction techniques. *Journal of Statistical Computation and Simulation* 1986; **23**:183–209.
33. Rosenblatt M. Remarks on a multivariate transformation. *Annals of Mathematical Statistics* 1952; **23**:470–472.
34. Abramowitz M, Stegun IA. *Handbook of Mathematical Functions* (9th edn). Dover Publications, Inc.: New York, NY, 1972.
35. Davenport WB, Root WL. *An Introduction to the Theory of Random Signals and Noise*. McGraw-Hill: New York, 1958.

## ERRATUM

### A generalized dimension-reduction method for multi-dimensional integration in stochastic mechanics (*Int. J. Numer. Meth. Engng* 2004; **61**:1992–2019)

H. Xu and S. Rahman

*Department of Mechanical and Industrial Engineering, The University of Iowa, 2140 Seamans Center,  
 Iowa city, IA 52242-1527, U.S.A.*

In Example 6, the results listed in Table VI of the above article were obtained when the covariance function  $\Gamma_\alpha(\xi) = \sigma_\alpha^2 \exp[-(|\xi_1| + |\xi_2|)/(bL)]$ ,  $\forall \mathbf{x}, \mathbf{x} + \xi \in \Omega$ . For the isotropic covariance function described by Equation (48), the corrected Table VI should read:

Table VI. Standard deviations of displacement and strains in plate with a hole by various methods ( $N = 12$ ).

Location	Response variable*	Standard deviation of response			
		4th-Order Neumann expansion method	Univariate dimension-reduction method	Bivariate dimension-reduction method	Monte Carlo simulation (5000 samples)
A	$u_1$	$1.17 \times 10^{-1}$	$1.15 \times 10^{-1}$	$1.17 \times 10^{-1}$	$1.19 \times 10^{-1}$
	$\varepsilon_{11}$	$2.78 \times 10^{-2}$	$2.72 \times 10^{-2}$	$2.78 \times 10^{-2}$	$2.79 \times 10^{-2}$
	$\varepsilon_{22}$	$2.57 \times 10^{-1}$	$2.51 \times 10^{-1}$	$2.57 \times 10^{-1}$	$2.58 \times 10^{-1}$
	$\varepsilon_{12}$	$3.52 \times 10^{-2}$	$3.45 \times 10^{-2}$	$3.52 \times 10^{-2}$	$3.54 \times 10^{-2}$
B	$u_1$	$4.92 \times 10^{-1}$	$4.83 \times 10^{-1}$	$4.93 \times 10^{-1}$	$4.95 \times 10^{-1}$
	$\varepsilon_{22}$	$8.58 \times 10^{-2}$	$8.41 \times 10^{-2}$	$8.59 \times 10^{-2}$	$8.49 \times 10^{-2}$
C	$u_2$	$2.64 \times 10^{-1}$	$2.58 \times 10^{-1}$	$2.64 \times 10^{-1}$	$2.66 \times 10^{-1}$
	$\varepsilon_{11}$	$9.12 \times 10^{-2}$	$8.92 \times 10^{-2}$	$9.13 \times 10^{-2}$	$9.28 \times 10^{-2}$
	$\varepsilon_{22}$	$1.38 \times 10^{-2}$	$1.35 \times 10^{-2}$	$1.38 \times 10^{-2}$	$1.41 \times 10^{-2}$
	$\varepsilon_{12}$	$4.06 \times 10^{-2}$	$3.97 \times 10^{-2}$	$4.07 \times 10^{-2}$	$4.13 \times 10^{-2}$
D	$u_2$	1.44	1.41	1.44	1.44
	$\varepsilon_{22}$	$8.76 \times 10^{-2}$	$8.53 \times 10^{-2}$	$8.77 \times 10^{-2}$	$8.52 \times 10^{-2}$
E	$u_1$	$6.03 \times 10^{-1}$	$5.91 \times 10^{-1}$	$6.04 \times 10^{-1}$	$5.98 \times 10^{-1}$
	$u_2$	1.46	1.44	1.47	1.46
	$\varepsilon_{22}$	$8.74 \times 10^{-2}$	$8.53 \times 10^{-2}$	$8.76 \times 10^{-2}$	$8.59 \times 10^{-2}$

\*  $u_1$  and  $u_2$  are horizontal and vertical displacements, respectively.  $\varepsilon_{11}$  and  $\varepsilon_{22}$  represent normal tensorial strains in  $x_1$  and  $x_2$  directions, respectively; and  $\varepsilon_{12}$  represents tensorial shear strain.

The authors apologize for any inconvenience caused.